energies

MDPI

Review

Hydrogen Combustion: Features and Barriers to Its Exploitation in the Energy Transition

Eugenio Giacomazzi *,†,‡, Guido Troiani ‡, Antonio Di Nardo ‡, Giorgio Calchetti ‡, Donato Cecere ‡, Giuseppe Messina ‡ and Simone Carpenella ‡

Laboratory of Processes & Systems Engineering for Energy Decarbonisation, ENEA, Via Anguillarese 301, 00123 Rome, Italy; guido.troiani@enea.it (G.T.); antonio.dinardo@enea.it (A.D.N.); giorgio.calchetti@enea.it (G.C.); donato.cecere@enea.it (D.C.); giuseppe.messina.cas@enea.it (G.M.); simone.carpenella@enea.it (S.C.)

* Correspondence: eugenio.giacomazzi@enea.it

† Current address: Casaccia Research Center, TERIN-PSU-IPSE, S.P. 081, ENEA, Via Anguillarese 301, S.M. Galeria, 00123 Rome, Italy.

‡ These authors contributed equally to this work.

Abstract: The aim of this article is to review hydrogen combustion applications within the energy transition framework. Hydrogen blends are also included, from the well-known hydrogen enriched natural gas (HENG) to the hydrogen and ammonia blends whose chemical kinetics is still not clearly defined. Hydrogen and hydrogen blends combustion characteristics will be firstly summarized in terms of standard properties like the laminar flame speed and the adiabatic flame temperature, but also evidencing the critical role of hydrogen preferential diffusion in burning rate enhancement and the drastic reduction in radiative emission with respect to natural gas flames. Then, combustion applications in both thermo-electric power generation (based on internal combustion engines, i.e., gas turbines and piston engines) and hard-to-abate industry (requiring high-temperature kilns and furnaces) sectors will be considered, highlighting the main issues due to hydrogen addition related to safety, pollutant emissions, and potentially negative effects on industrial products (e.g., glass, cement and ceramic).

Keywords: hydrogen combustion; hydrogen blends; power generation; gas turbines; hard-to-abate industry

Citation: Giacomazzi, E.; Troiani, G.; Di Nardo, A.; Calchetti, G.; Cecere, D.; Messina, G.; Carpenella, S. Hydrogen Combustion: Features and Barriers to Its Exploitation in the Energy Transition. *Energies* **2023**, *16*, 7174. https://doi.org/10.3390/en16207174

Academic Editors: Samuel Simon Araya and Liso Vincenzo

Received: 25 September 2023
Revised: 16 October 2023
Accepted: 19 October 2023
Published: 20 October 2023

1. Introduction

According to the International Energy Agency, energy efficiency, behavioral change, electrification, renewables, hydrogen and hydrogen-based fuels, and carbon capture, utilization, and storage (CCUS) are the key pillars to decarbonizing the global energy system [1]. The increasing share in cumulative emission reductions due to hydrogen justifies its important role in the net zero emissions scenario [1] to decarbonize sectors where emissions are hard to abate, such as heavy industry and long-distance transport. Within the power sector, hydrogen holds the potential to deliver flexibility by aiding in the management of increasing proportions of fluctuating renewable energy generation. Additionally, it can play a role in enabling seasonal energy storage, further enhancing the versatility and reliability of the energy system.

Hydrogen stands out as an exceptionally versatile fuel that can be generated using a wide spectrum of energy sources, encompassing coal, oil, natural gas, biomass, renewables, and nuclear power. The production methods are equally diverse, spanning processes like reforming, gasification, electrolysis, pyrolysis, water splitting, and numerous others. In recent times, distinct colors have been assigned to signify different pathways of hydrogen production: "green" for hydrogen extracted through electrolysis with electricity from renewable sources; "grey" for H_2 produced from fossil raw materials such as natural gas (this generates around 10 tons of CO_2 per ton of H_2); "blue" for production derived

from fossil fuels with CCUS; "turquoise" for H_2 produced by splitting natural gas at high temperatures (only solid carbon is produced in the process, i.e., no CO_2 is emitted if the process runs on heat from renewable energy sources). Due to the multitude of energy sources that can be employed, the environmental consequences associated with each method of hydrogen production can differ significantly. Moreover, the geographic location and the specific configuration of the process also play a crucial role in shaping these environmental impacts.

As of 2020, the worldwide demand for hydrogen amounted to approximately 90 million metric tons (Mt) [1], indicating a growth of 50% since the year 2000. Nearly the entirety of this demand is attributed to applications in refining and industrial sectors. Refineries, on an annual basis, utilize nearly 40 million metric tons of hydrogen for tasks such as feedstock and reagents, as well as an energy source.

Demand is slightly elevated in the industrial sector, surpassing 50 million metric tons (Mt) of hydrogen [1]. This demand is primarily attributed to its use as feedstock. Within the chemical production sector, approximately 45 million metric tons of hydrogen are consumed, with roughly three-quarters allocated to ammonia production and the remaining one-quarter directed towards methanol production. The remaining 5 million metric tons of hydrogen find usage in the direct reduced iron (DRI) process for steelmaking. This allocation of demand has remained nearly unchanged since 2000, with only a marginal uptick in demand noted for DRI production.

Simultaneously, mounting concerns about climate change have led to heightened awareness, prompting both governments and industries to make resolute pledges aimed at curtailing emissions. While this has expedited the integration of hydrogen into novel applications, the demand in this realm still remains quite limited. For instance, in the transport sector, the yearly hydrogen demand stands at less than 20 thousand metric tons (kt) of hydrogen, representing a mere 0.02% of the overall hydrogen demand. As illustrated in the IEA roadmap for achieving a net-zero state by 2050 [2], achieving government decarbonization objectives will necessitate a significant and abrupt acceleration in the adoption of hydrogen technologies across various segments within the energy sector.

In the net zero emissions scenario [2], the demand for hydrogen experiences a substantial increase, expanding nearly six times its current value to reach 530 million metric tons (Mt) of hydrogen by the year 2050. This surge in demand is divided, with half of it being allocated to the industry and transport sectors. In this scenario, the presence of hydrogen in the power sector undergoes a marked increase. Its utilization in gas-fired power plants and stationary fuel cells plays a crucial role in mitigating the challenges associated with the growing output from variable renewable sources, facilitating the integration of larger proportions of solar photovoltaic (PV) and wind energy, and furnishing seasonal energy storage solutions. Additionally, hydrogen's application in buildings also encounters growth, although its adoption remains constrained to specific circumstances. In the same scenario projected for 2050, approximately one-third of the hydrogen demand is allocated to the production of hydrogen-based fuels. These fuels include ammonia, synthetic kerosene, and synthetic methane. Current applications of ammonia are primarily centered around nitrogen fertilizers, but now the interest is growing in other sectors, such as the long-distance shipping of hydrogen and combustion, where the co-firing of ammonia in coal-fired power plants has shown successful demonstrations; however, further research, development, and deployment efforts are necessary to advance the utilization of pure ammonia as a direct fuel source (also thermally and catalytically decomposed) in steam or gas turbines [3].

When hydrogen is burned, the primary resultant is water (H_2O), rendering it a genuinely emission-free fuel in terms of CO_2. The ultimate objective is to utilize 100% green hydrogen for combustion, entirely supplanting natural gas. In the interim, a more immediate goal involves blending hydrogen with natural gas to be used in gas turbines and other industrial combustion applications, thereby achieving a partial reduction in CO_2 emissions. Nowadays, the term fuel-flexibility refers to combustion-based power generation system

(especially gas turbines) capabilities to operate with hydrogen blends as fuel in a stable, safe, and reliable way when the H_2 content unpredictably varies in time due to intermittent production from renewables. Such blends range from hydrogen-enriched natural gas (HENG) to ammonia (a promising H_2-carrier).

An important but frequently overlooked factor that is easily comprehensible is the necessity for a substantial proportion of hydrogen by mass in fuel mixtures to produce a noteworthy impact on CO_2 emissions. It is common to discuss these proportions in terms of volume fractions, but in the context of methane/hydrogen blends, the volume percentage of H_2 significantly differs from its mass equivalent, as illustrated in Figure 1. For instance, 30% and 50% volume correspond to just 5% and 11% mass, while achieving an emission reduction of 55% necessitates an 80% volume fraction. Nevertheless, even maintaining a low 30% volume fraction becomes quite challenging when factoring in significant temporal fluctuations in composition.

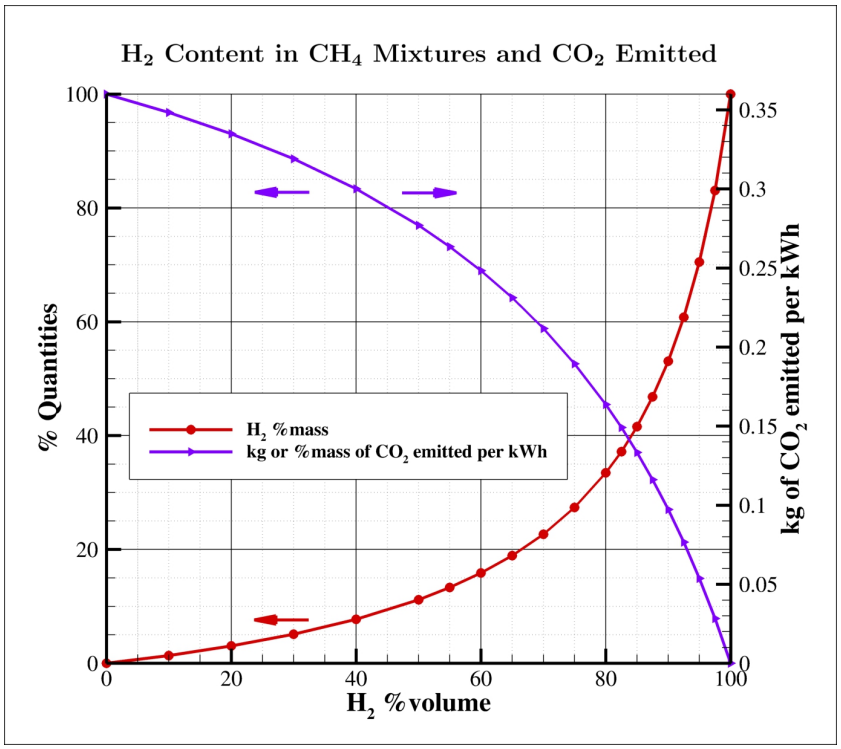

Figure 1. Correlation between volume and mass percentages within methane/hydrogen blends, and its consequential effect on CO_2 emissions (considering an assumed electrical efficiency of 55% in the computation). The percentage values on the left are in reference to pure methane.

Adopting hydrogen in combustion application is not straightforward. A fuel consisting in 100% hydrogen necessitates an extra volumetric flow of 208%, approximately three times more than that needed for methane to have the same power; hence, depending on the blend percentage, there might be a need to expand the size of piping and valves to manage the higher volumetric flow demanded by hydrogen. Its physical characteristics introduce complexities in terms of production, storage, and transportation, setting it apart from natural gas. Safety issues also arise due to hydrogen's broader flammability range, lower vapor density, and faster flame speed, necessitating careful consideration within the framework of system design. Safety mechanisms for gas detection and fire protection must be adjusted to address hydrogen's unique volatility and distinctive detection characteristics. Correspondingly, measures for explosion-proofing should be equipped to confine more substantial explosions, and modifications to ventilation systems are essential. Moreover, hydrogen encounters distinctive challenges related to supply and infrastructure. The fuel system's pipelines and valves enclosed must harmonize with hydrogen, necessitating mate-

rials that are hydrogen-compatible and designed with safety factors in mind. Additionally, the design must incorporate hydrogen-tight seals capable of accommodating the small hydrogen gas molecules.

In this article, the combustion features of hydrogen enrichment in fuel blends will be firstly considered, also briefly looking at the effects on materials. Then, an overview of combustion applications in power generation and hard-to-abate sectors will be provided to identify the state-of-the-art and the barriers for its exploitation. In the end, conclusions and future directions will be drawn.

2. Features of Hydrogen Combustion

When employing hydrogen either alongside natural gas or as a complete substitute, it is crucial to grasp the distinctions between these two fuels.

Hydrogen possesses a density that is one-ninth that of natural gas, and it holds the distinction of being the smallest known molecule. This characteristic introduces challenges regarding transportation and sealing. Furthermore, hydrogen's heating value is merely one-third that of natural gas (on a volumetric basis), signifying that three times the amount of hydrogen fuel is necessary to generate an equivalent power output compared to natural gas. In hydrogen combustion, although a higher volume flow of fuel is needed for equivalent energy production, about 20% less air by volume is necessary to generate a flame comparable to natural gas. This reduction in the air volume requirement results in a decreased mass flow through the combustor, subsequently reducing convective heat transfer. From this standpoint, flue gas recirculation can be employed to increase the mass flow of air into the combustor, thereby increasing convective heat transfer and lowering the flame temperature, as discussed in [4–6].

Moreover, hydrogen has a considerably broader flammability range than natural gas, leading to heightened concerns regarding environmental, health, and safety aspects during both hydrogen transportation and combustion. Although it has recently been observed [7] that mixtures containing higher H_2 concentrations are slower to ignite compared to those with higher CH_4 concentrations at low temperatures (below 930 K, for hydrogen combustion, the self-recombination of HO_2 radicals leads to chain propagation which inhibits reactivity, whereas for methane combustion, the reaction between radicals and HO_2 leads to chain branching, increasing reactivity), for higher temperatures hydrogen largely enhances the reactivity of fuel blends: the ignition delay time decreases [8–11]; at room temperature and pressure, the flammability limits (0.1–7.1) are well wider than those of natural gas (0.5–1.67); the flame speed is higher [12] and the critical strain rate increases, thus reducing potential flame quenching [13,14]. At a fixed equivalence ratio (Φ), the hydrogen/air premixed flame burns with an adiabatic flame temperature higher than the corresponding natural gas one (see Figure 2, left). In the same way, fixing the equivalence ratio, the increase in the hydrogen content in a methane/hydrogen mixture can rise the adiabatic flame temperature (see Figure 2, right).

Figure 3 reports data on laminar and turbulent flame speed from [15,16] for CH_4/H_2 fuel mixtures with hydrogen content up to 50% vol. The data are specific to lean premixed fuel/air mixtures ($0.4 < \phi < 0.5$) at 5 bar, preheated at 673 K, flowing at 40 m/s, and with a 15% inlet turbulence intensity. Laminar flame speed values were calculated based on the GRI3.0 chemical mechanism. The data on turbulent flame speed show the unexpected effects of increasing the hydrogen content. Initially, there is a moderate, nearly linear increase in turbulent flame speed, following the trend of calculated laminar flame speed, but the linearity varies with the equivalence ratio, is longer for leaner mixtures. This suggests complex interactions between hydrogen addition and combustion properties. The differences (evident in the richer mixtures in Figure 3) highlight the presence of both the chemical kinetics and physical (diffusivity, thermal conductivity, turbulence) effects of the hydrogen addition: the linear trends depict the chemical kinetics reaction properties of the fuel gas mixtures; beyond the limits of the linear region, the turbulent flame speed rapidly diverges (similar trends are observed for the leaner conditions but shifted towards

higher hydrogen concentrations). Hence, besides the chemical kinetics effects influenced by hydrogen, which are reflected in changes in the laminar flame speed, the physical properties of hydrogen also accelerate the consumption rate of the fuel species. One of the physical effects is that the presence of hydrogen in air/hydrocarbon blends, especially at the leaner equivalence ratios, decreases the Markstein length, even to negative values [17,18]. Thus, a positively stretched flame increases its laminar combustion velocity, in contrast to a pure hydrocarbon/air flame (with a positive Markstein number along its whole flammability limit), whose laminar combustion velocity is increased when negatively stretched. The increase in hydrogen content is shown to lower the thickness of the flame pre-heat zone, while the heat release zone seems to be insensitive to turbulence effects, at least in the broadened preheat-thin reaction zone [19]. Some other physical effects of the hydrogen addition will be discussed in Section 2.1.

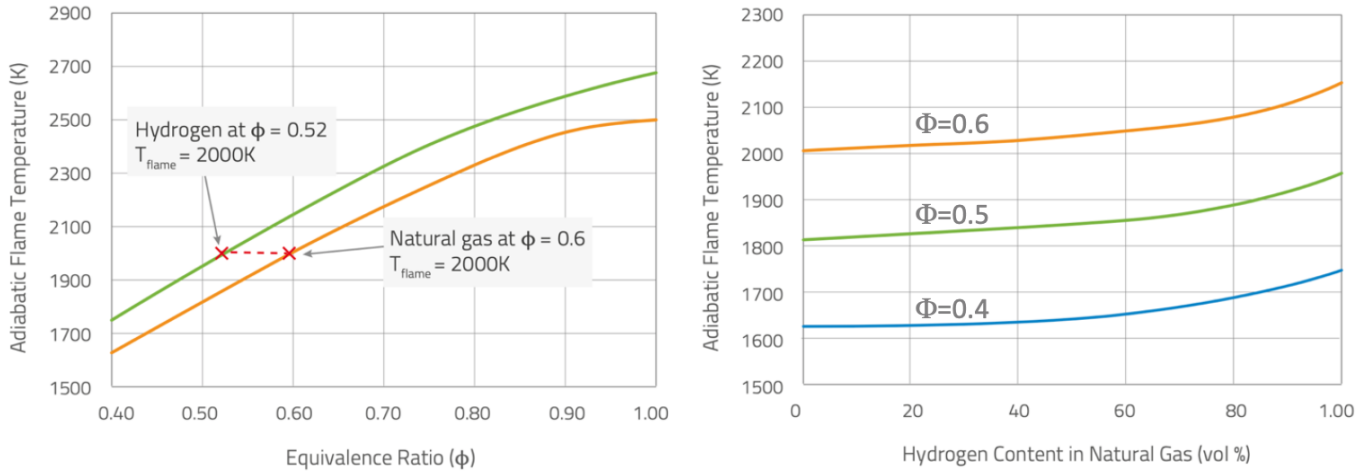

Figure 2. Adiabatic flame temperature vs. equivalence ratio (Φ) for hydrogen and methane flames in air (**left**), and vs. hydrogen content for some specific mixtures (**right**) [15].

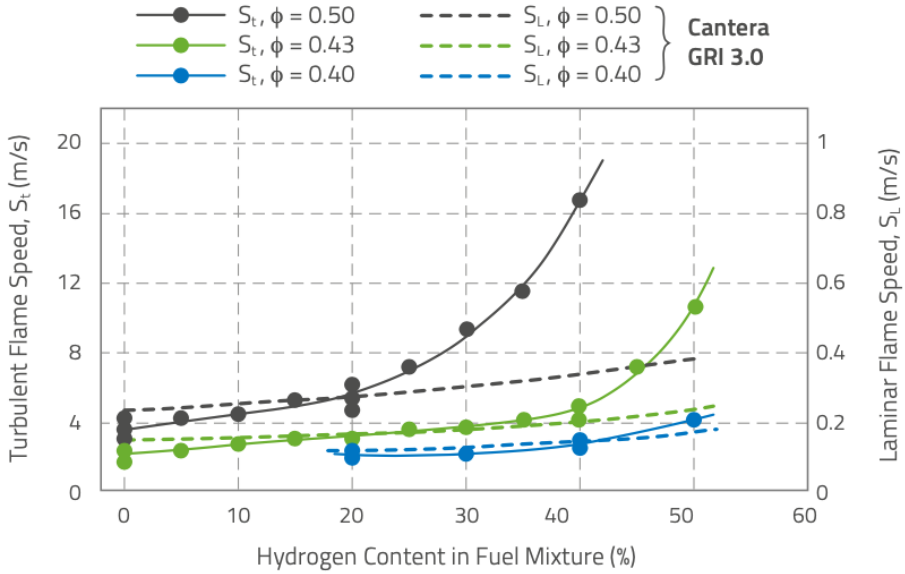

Figure 3. Laminar and turbulent flame speed for CH_4/H_2 fuel mixtures with different hydrogen from [15]. Laminar flame speed data come from chemical kinetics calculations based on the GRI3.0 chemical mechanism. Turbulent flame speeds come from experimental measurements.

The higher hydrogen combustion temperatures produce an increase in nitrogen oxides, NO_x, most of which is thermal, i.e., coming from high-temperature regions with sufficiently long residence times [20]. This is one of the main concerns in operating burners with fuel

blends having a high H_2 content. Also, turbulence plays its role in the formation of NO_x, e.g., they are reduced as the Karlovitz number and the H_2 content are increased, and the turbulent flame brush thickened [21].

Being a fundamental aspect in any combustion process, chemical kinetics is now embraced as a closing topic in this introduction on hydrogen characteristics. Detailed chemical kinetics mechanisms are effective in computing the key properties of simplified flames, including adiabatic flame temperature, flame speed, and autoignition delay time. Moreover, they find use in fluid dynamics calculations that aim to simulate actual combustion systems. Since such simulations become excessively demanding when coupled with detailed chemistry and the transport of each individual species involved in the chemical mechanism adopted, real-world combustion systems can be represented through a network of simplified chemical reactors, where very detailed chemistry can be applied [22].

Hydrogen reactions play a central role in the combustion kinetics of any fuel. Specifically in the context of hydrogen combustion, the Konnov mechanism [23,24] has been recently developed, also in conjunction with carbon chemistry. These mechanisms are highly detailed and exhibit good agreement with experimental data, as well as with other significant kinetic models. In [23], a comparison was made between experimental and computational results employing two modern and comprehensive chemical kinetic mechanisms, Glarborg [25] and POLIMI [26]. Discrepancies were observed, particularly at rich equivalence ratios, but the Konnov model [23] demonstrated a strong overall performance in replicating laminar burning velocities and NO concentrations. At lean equivalence ratios, the adiabatic burning velocities from both numerical and experimental studies matched quite closely, with minor distinctions emerging under rich conditions, where the Konnov model aligned more closely with experimental values despite inherent uncertainties. In the prediction of NO levels, the Konnov model also came closest to experimental outcomes, displaying only slight deviations, primarily under rich conditions where other kinetic schemes underperformed. This superior performance in rich conditions was attributed to the Konnov model's better approximation of prompt, or Fenimore, NO_x formation. Nonetheless, it is worth noting that the Konnov mechanism is not the sole kinetic mechanism under consideration for hydrogen-containing fuels. The AramcoMech 1.3 mechanism [27] has been effectively used to predict autoignition delay times for hydrogen-containing mixtures [10]. Despite advancements in the development of chemical kinetic schemes, uncertainty persists regarding the optimal approach to describe the full spectrum of properties across various natural gas blends with hydrogen.

2.1. Effects on Flame Stability

Combustion in excess of air can mitigate NO_x production [28], but at these conditions of extremely lean combustion, the gaseous mixtures rich in hydrogen are characterized by a disparity between the diffusion by mass and the thermal one, inducing phenomena of intrinsic instability with a strong impact on the laminar and turbulent combustion speed, and thus altering the flame topology.

These effects have been theoretically predicted [29–31], as well as experimentally [32,33] and numerically visualized (numerical simulations) [34–36]. In particular, these reactive mixtures are extremely sensitive to some external perturbations (usually present in every burner) producing exponential growths in the extension of the flame front, in pressure fluctuations, as well as in temperature, with a negative impact on the performance of thermal machines, their polluting emissions, and even their life time. However, with an accurate design of the combustion chamber, it is possible to maximize the advantages deriving from these instabilities, i.e., the increase in the average combustion speed (and therefore, in the thermal power) and compactness of flames (smaller size of the devices), while eliminating or mitigating the negative aspects, such as high pressure and temperature fluctuations, localized quenching and flashbacks.

Hydrogen, and light species in general, diffuse preferentially with respect to other species in a mixture. In recent decades, so-called asymptotic theories [29–31] have been

developed which predict the existence of perturbations (in specific wavelength ranges) that are particularly effective in destabilizing combustion processes, which strongly depend on the Lewis number of the mixture. The Lewis number (Le) represents a measure of the disparity between thermal and mass diffusivity, through their ratio: therefore, a hydrogen-rich mixture, which has a mass diffusivity that is extremely greater than the methane molecule, will be characterized by a Lewis number less than unity. In a premixed combustion, this makes the local equivalence ratio lower or higher than the inlet nominal equivalence ratio of the considered fuel blend depending on the local flame curvature. An example is provided in Figure 4 for a CH_4/H_2—air flame at a nominal $\Phi = 0.7$ and 20% H_2 volume content [37], where the instantaneous flame surface (identified by means of the progress variable value related to the maximum heat release) is shown, evidencing local hydrogen enrichment in positive curvature regions, and a decrease in the equivalence ratio in negative curvature regions. This mechanism changes flame speed locally, and tends to enhance the wrinkling of the flame front and the burning rate.

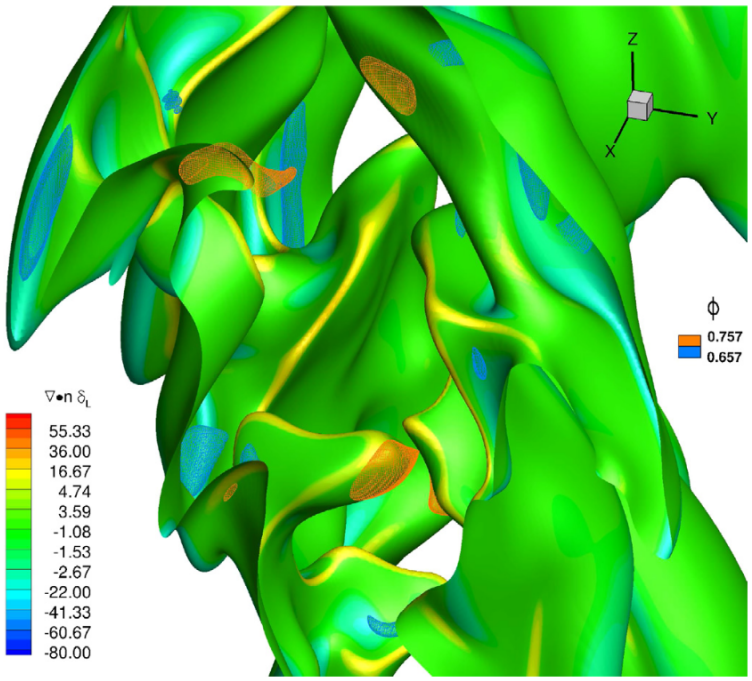

Figure 4. Snapshot of a progress variable iso-surface associated to the maximum heat release colored with its normalized curvature and two iso-surfaces of equivalence ratio at $\Phi = 0.657$ (blue) and $\Phi = 0.757$ (orange), respectively, for a CH_4/H_2—air flame at a nominal $\Phi = 0.7$ and $X_{H_2} = 0.2$ [37].

Mixtures with Lewis numbers smaller than a critical value (Le_c, generally less than one) will be characterized by small-scale (thermo-diffusive) and large-scale (hydro-dynamic) instabilities. With a Lewis number close to the Le_c or greater, mainly hydro-dynamic instabilities will survive. This type of instability is based on different formation mechanisms. In the case of thermo-diffusive instabilities, the high diffusivity of the mixture (in particular of H_2) will give rise, when the flame front is perturbed/corrugated, to inhomogeneity of the equivalence ratio of the mixture and of the local temperatures with a consequent variation of the local laminar combustion speeds, which in turn will amplify the initial perturbations of the front, making it even more corrugated. Such corrugations increase the turbulent flame speed, as shown in Figure 5, that reports the ratio between the turbulent and laminar flame speeds of a premixed $CH_4/H_2/Air$ Bunsen flame: the lower the Lewis number and the higher the turbulence intensity, the higher the turbulent flame speed will be [38,39].

This phenomenon is more effective with more perturbations, and the corrugations of the front are small in scale. In the case of $Le > Le_c$, this phenomenon is strongly limited, and what arises is a hydro-dynamic type mechanism, in which the large-scale corrugations

of the front compress or expand the stream lines of the flow field, thus channeling areas with low or high velocity upstream of the flame front. Also, this mechanism initially tends to amplify small-amplitude perturbations.

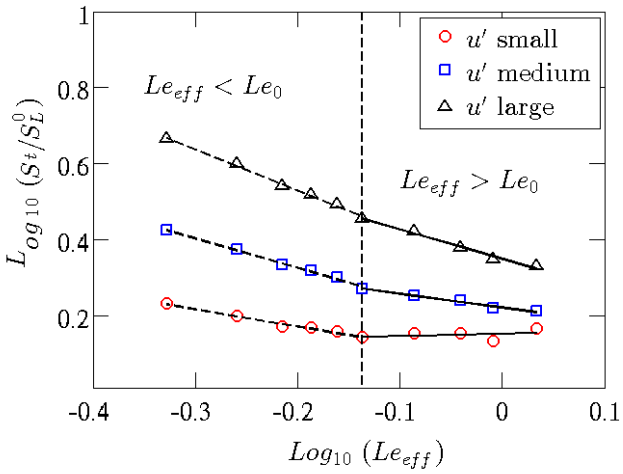

Figure 5. Ratio between turbulent and laminar flame speeds versus the effective Lewis number, as defined in [40], in a premixed $CH_4/H_2/Air$ Bunsen flame, parameterized with turbulence intensity of the jet, from studies in [38,39].

The presence of thermo-diffusive instabilities alone is not possible. In fact, since the a phenomenon of hydro-dynamic instability is always present in a flame, due to the difference in temperature between reactants and combustion products, that of the thermo-diffusive type is driven by the disparity between the mass and thermal diffusivity, which can be eliminated by acting on the composition of the reactant mixture. Studies present in the literature have shown the interaction, in Bunsen geometries, of hydrodynamic instabilities with flow turbulence [41–45], while the characterization of the interaction of turbulence with both instabilities (hydro-dynamic and thermo-diffusive) still lacks.

Due to its elevated combustion temperature and faster flame speed, hydrogen combustion presents an increased susceptibility to instability, potentially leading to flameouts and flashback incidents. Specifically, the heightened reactivity of hydrogen inherently raises the risk of self-ignition and flashbacks, primarily within the premix section. This concern becomes even more critical in systems characterized by exceedingly high inlet air temperatures, such as those found in highly recuperated gas turbines, as referenced in [46,47]. Furthermore, hydrogen flames exhibit a substantially different thermoacoustic behavior compared to natural gas flames, owing to their higher flame velocity, shorter ignition delay, and distinct flame stabilization mechanisms. These differences result in varying flame shapes, positions, and reactivity. Consequently, the potential for combustion dynamics, characterized by self-sustained oscillations at the acoustic frequency of the combustion chamber, is higher in gas turbines running on hydrogen-enriched fuels than in natural gas operation, as indicated in [48,49]. This implies that undesired and hazardous phenomena, such as combustion instability, flashbacks, and lean-blowouts, can manifest not only during steady-state operation but also during transient regimes. For instance, these issues may arise when the power output changes rapidly or when the fuel composition undergoes variations.

2.2. Effects on Pollutant Emissions

The main emission indicators on which the performance of burners are based are mainly the nitrogen oxides NO_x, composed of NO and NO_2, CO and carbon dioxide CO_2.

There is no fundamental chemical kinetic reason why H_2 flames should produce more NO_x than natural gas flames. Since most NO_x is thermal, i.e., produced where reactants are at a high temperature for a sufficiently long residence time (above a certain threshold

temperature, around 1800 K, the production of NO_x increases dramatically), more lean mixtures have to be adopted to reduce the peak temperatures (see Figure 2) when burning fuel blends with higher a H_2 content.

Figure 6 (top) shows a map of NO_x emissions as a function of the equivalence ratio and hydrogen content for a CH_4/H_2 blend reacting with air at two different pressures [50]: respecting NO_x emission limits requires that one operates at an equivalence ratio well below 0.5, especially at high H_2 content and high pressure. The implementation of exhaust gas recirculation (EGR) can be of help in reducing NO_x emissions in different applications (see Figure 6, bottom), and in gas turbines, it is a potential solution to enhance their turn-down ratio, i.e., to reduce their partial load (minimum technical environmental load).

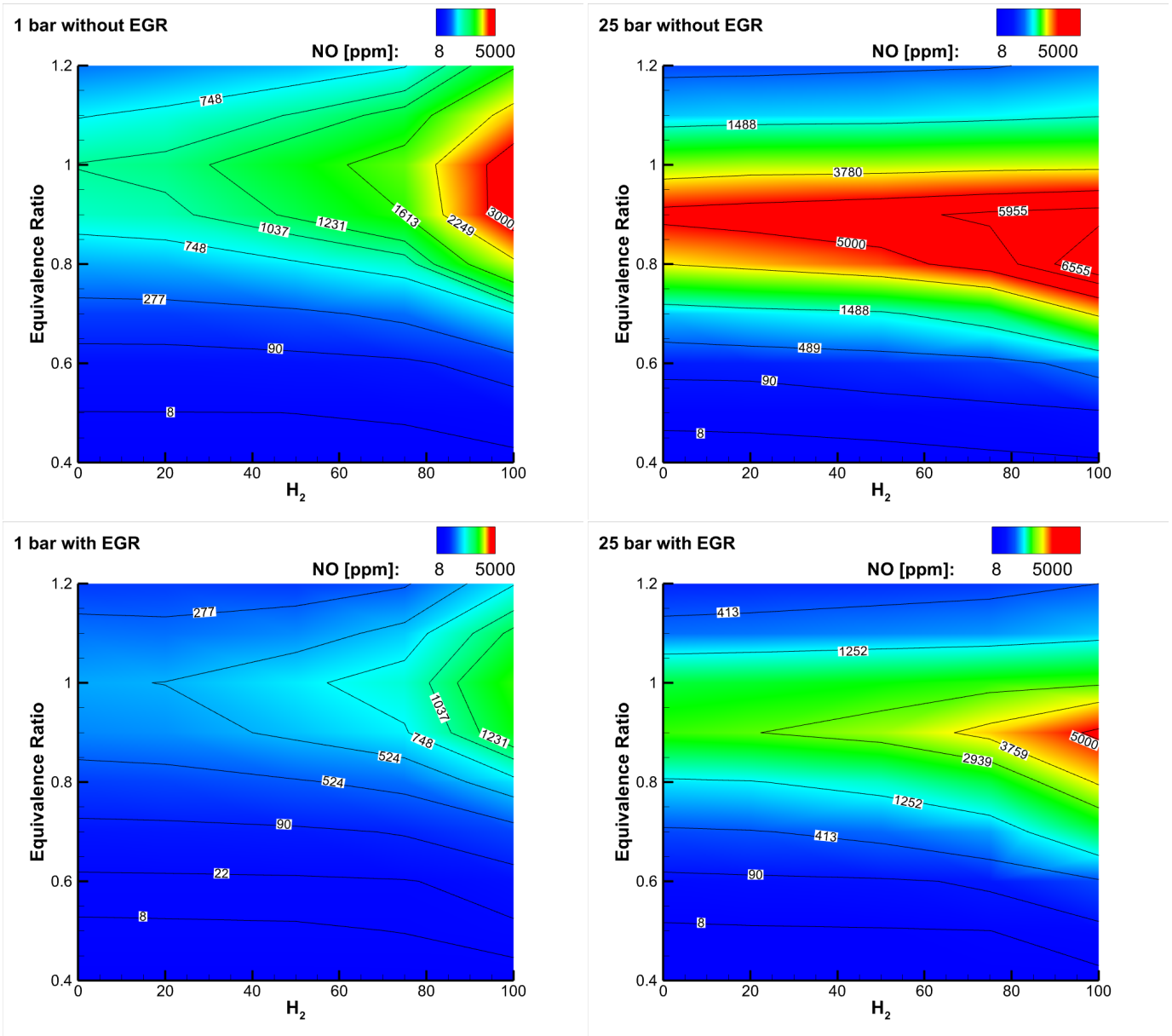

Figure 6. NO_x emissions in ppm vs. equivalence ratio and hydrogen content for a CH_4/H_2 blend reacting with air without and with dilution through exhaust gas recirculation (EGR). Two pressures are considered: 1 bar (**left**) and 25 bar (**right**). The initial temperature of reactants changes with the hydrogen content: without EGR, it is in the range of 750–820 K, and with EGR, it is in the range of 800–850 K, decreasing while H_2 is increased [50].

Apart from NO_x predictions and expectations from chemical kinetics calculations, some direct measurements of NO_x emissions in a specific premixed Bunsen burner at 1 atmosphere are here reported due to the interesting operational strategy implemented to avoid flashback occurrence [39]: as the hydrogen content increases in the CH_4/H_2 fuel blend, driving the increase in flame propagation speed, the value of the equivalence ratio is decreased by increasing the excess air. This strategy allowed to maintain the flame propagation speed constant (0.33 m/s), and at the same time, lowered the adiabatic flame temperature; additionally, the power was kept constant (7.1 kW) by raising the flow rate of the reactant mixture. Such a strategy avoided a flashback up to the maximum jet Reynolds number (explored range, 10.000–13.900) in [39]: it would be interesting to see what happens at higher turbulent jet Reynolds numbers to check the effects on the nonlinear increase in the turbulent flame speed. The measurements of emissions were carried out at the chimney, taking a small quantity of combustion products and analyzing them by means of the FTIR (Fourier transform infrared spectroscopy) technique [51,52].

Figure 7 shows the quantity of NO_x expressed in parts per million (ppm), scaled to a value of oxygen in the combustion equal to 15%, as well as in mass normalized by the fuel energy actually converted into heat, to take into account the different composition of exhausts while increasing the hydrogen content [39]. Additionally, in this way, the emission values of machines of significantly different sizes (power) can be compared. It is observed that, above a hydrogen mole fraction of 45–50%, emissions decrease dramatically. This is due to the regulation strategy adopted in [39]: while the hydrogen content is increased, the equivalence ratio is decreased, thus lowering the flame temperature and thermal NO_x contribution (the most relevant). In fact, the temperature changes from about 2100 K for the methane flame to nearly 1600 K for the hydrogen one.

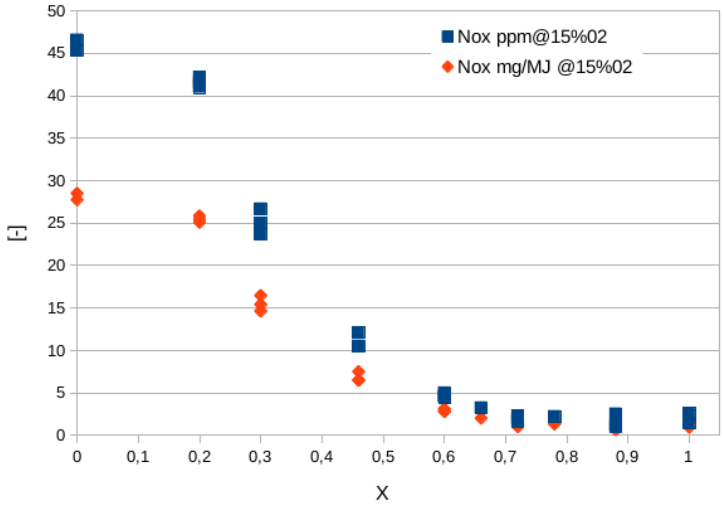

Figure 7. NO_x concentration in ppm (blue squared symbols) and mg/MJ (red diamonds) as the hydrogen content (expressed in molar fraction, *X*) varies in the premixed CH_4/H_2/Air Bunsen flames studied in [39]. Values are scaled at an oxygen content of 15%.

Figure 8 shows the results of the sampling of the carbon dioxide emitted in the same experiment [39]. As the percentage of hydrogen expressed as molar fraction increases (0, pure methane; 1, pure hydrogen), the carbon dioxide content drops until it reaches zero when the mixture is made up of only hydrogen and air. The results are in agreement with the chemiluminescence emission described later in Figures 11 and 12. As expected from the numerical calculation data in Figure 1, the presence of carbon dioxide is significant, even at very high H_2 mole fraction values.

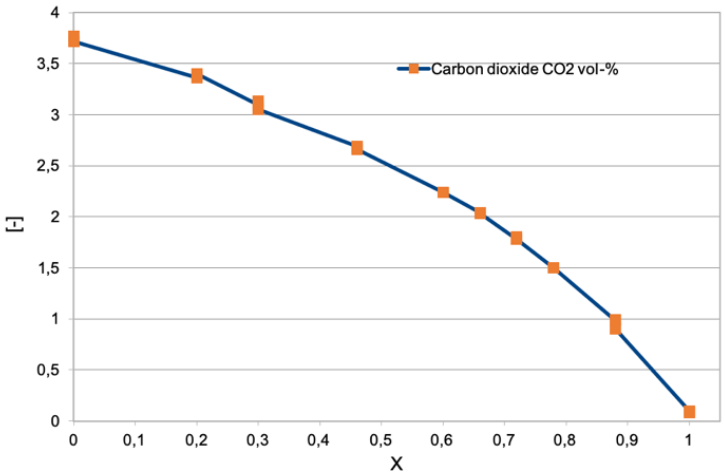

Figure 8. CO_2 concentration at varying hydrogen contents (the molar fraction is reported on the horizontal axis) in the premixed $CH_4/H_2/Air$ Bunsen flames studied in [39].

2.3. Effects on Radiant Energy Transfer

Radiative transfer of energy (RTE) is a highly significant mechanism in a multitude of applications, including high-pressure and high-temperature engine combustion chambers, rocket propulsion, hypersonic vehicles, spacecraft atmospheric reentry, ablating thermal protection systems, glass manufacturing, plasma generators, and nuclear fusion.

It is important to note that hydrogen flames are notably less visible compared to flames produced by natural gas. This reduced visibility is a result of the lower concentration of radiant species, including soot, CO_2, and radicals in hydrogen flames. Consequently, detecting these flames presents a more intricate challenge. Infrared flame detection methods are ineffective for hydrogen flames, necessitating the use of ultraviolet systems, as discussed in [53–56].

At the same time, this also affects the radiative heat transfer from the flame, with important implications in some applications, such as glass furnaces. The lower emissivity and lower mass flow rate (less air is required while increasing the H_2 content to generate a flame comparable to natural gas, i.e., with the same heat release) of the combustor, therefore changing the heat transfer balance.

The radiative absorption properties hinge on the absorption coefficient, denoted by κ_λ. In gases, this coefficient often exhibits significant variations with respect to wavelength, temperature, and pressure. It also increases in direct proportion to the concentration of participating species. While solid surfaces can generally be assumed as opaque, the absorption or emission properties of gases exhibit irregularities within the wavelength domain, becoming particularly noteworthy at temperatures below a few thousand Kelvin. As the temperature increases, the absorption coefficient for cold lines diminishes, but hot lines emerge at higher wavelengths, slightly increasing the absorption coefficient. Elevating the pressure results in spectral line broadening, primarily due to molecular collisions [57]. This broadening leads to wider and more overlapping lines, especially at higher pressures, rendering the gas more "gray" or opaque. Consequently, the amplitude of the spectral absorption coefficient significantly increases, as depicted in Figure 9 and as also reported in [58,59] (p. 138). An appropriate and practical average absorption coefficient for characterizing the total emission from a volume element within an absorbing medium is the Planck mean absorption coefficient. This coefficient solely depends on local properties and can be tabulated. Presently, the Planck mean absorption coefficients, which were estimated in the past [57] (pp. 253–324), can be more accurately computed directly from high-resolution spectroscopic databases, such as HITRAN [60] and HITEMP [61], as demonstrated in the study by [62]. The newer databases tend to yield absorption coefficients that are generally

higher than those obtained using older databases, particularly at higher temperatures and pressures: Figure 9 (bottom right) shows this effect for carbon monoxide.

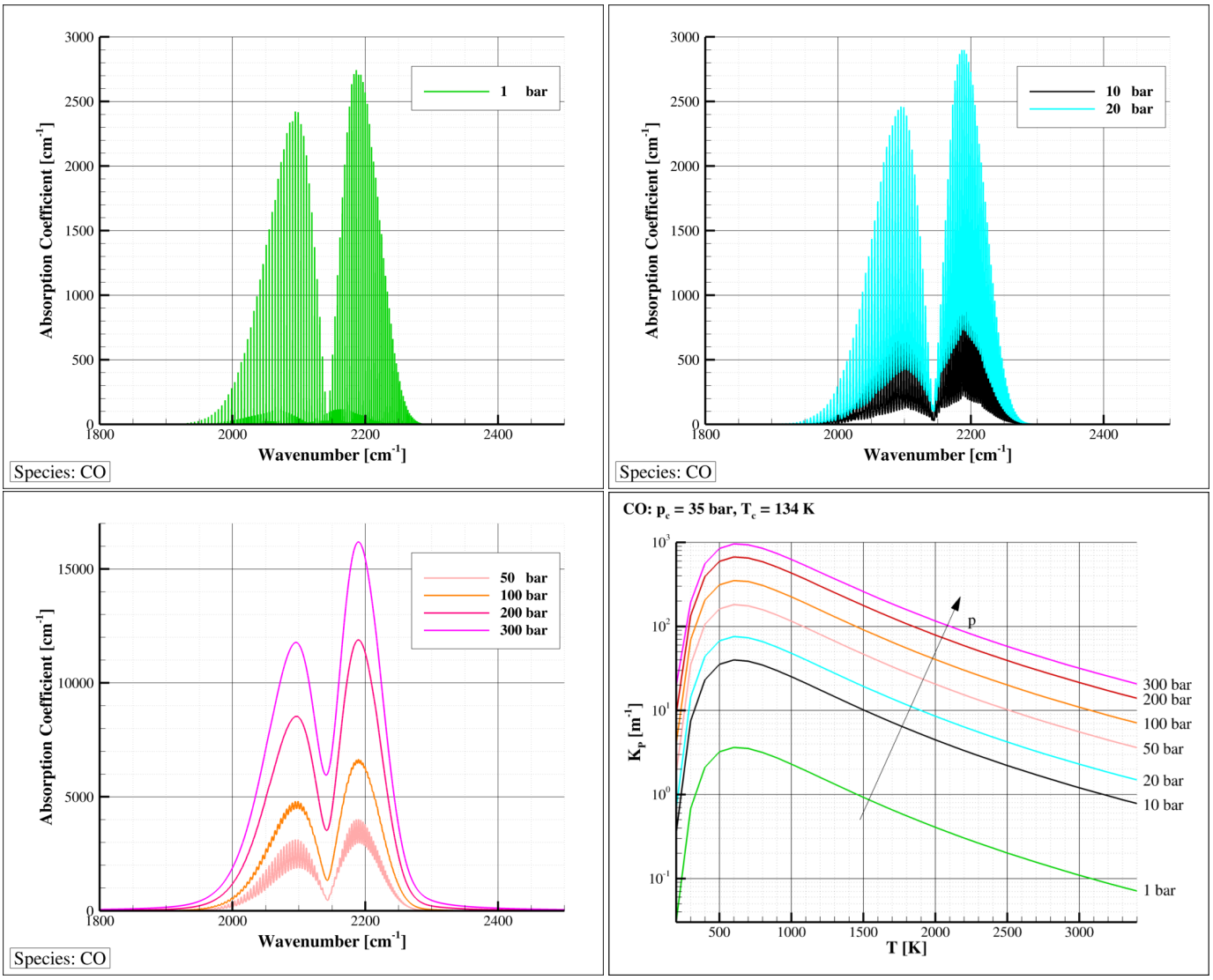

Figure 9. The carbon monoxide (CO) absorption coefficient at 800 K and different pressures (**top** and **bottom left**), and the related mean Planck absorption coefficient versus temperature (**bottom right**). Calculations were performed by means of the HAPI code [63] using the HITRAN [60] and HITEMP [61] high-resolution spectroscopic databases, with the Voigt model assumption for the line shape.

At the temperatures typically encountered in industrial furnaces and combustion chambers, the gaseous species that play a significant role in absorbing and emitting radiation are carbon dioxide (CO_2), water vapor (H_2O), carbon monoxide (CO), sulfur dioxide (SO_2), nitrogen oxide (NO), and methane (CH_4). Other gases, such as nitrogen (N_2), oxygen (O_2), and hydrogen (H_2), are essentially transparent to infrared radiation and do not significantly contribute to emission or absorption. However, their importance as absorbing and emitting contributors becomes pronounced at extremely high temperatures. Furthermore, a noteworthy contribution to radiation is also derived from hot carbon particles, commonly referred to as soot, within the flame, as well as from suspended particulate material, as is the case in pulverized-coal combustion processes.

Regarding flames, it is well established that disregarding radiation under atmospheric pressure conditions can result in an overestimation of temperature by as much as 200 K.

However, it is important to note that numerical predictions are highly dependent on the radiative transfer of energy (RTE) model employed. The commonly used optically thin or gray radiation models tend to underestimate the temperature by up to 100 K or more, as discussed in [64,65]. Moreover, radiation is intensified by turbulence through strong nonlinear interactions between fluctuations in temperature and radiative properties (TRI). These interactions lead to increased heat loss from a flame, resulting in a local gas temperature reduction of 200 K or more. This TRI cooling effect is even more pronounced in high-pressure combustors, which typically exhibit greater optical thickness, as highlighted in [66,67].

In systems where RTE is a significant factor, it has been demonstrated that radiation can be considered equivalent to a substantial nonlinear diffusion term. In fact, the transfer of heat through radiation can function as a preheating mechanism, similarly to heat conduction. As a result, this preheating effect contributes to higher flame speeds, as discussed in the work by Mercer in [68]. As an example, Figure 10 shows an instantaneous distribution of the radiative source term in the energy equation in a non-premixed cyclonic combustor [69] burning air and hydrogen in a MILD combustion regime. The source term is estimated by means of the M1-radiation model [70]: its distribution reveals regions exhibiting heat losses (negative radiative source term) or preheating effects (positive source). The distribution of the radiative source term versus temperature is also shown at the bottom of the same figure, colored by means of the OH radical mass fraction: regions reacting at higher temperatures with higher OH concentrations lose heat, while colder non-reacting regions (jets, identifiable in the planar section of Figure 10, top) with lower OH contents are preheated.

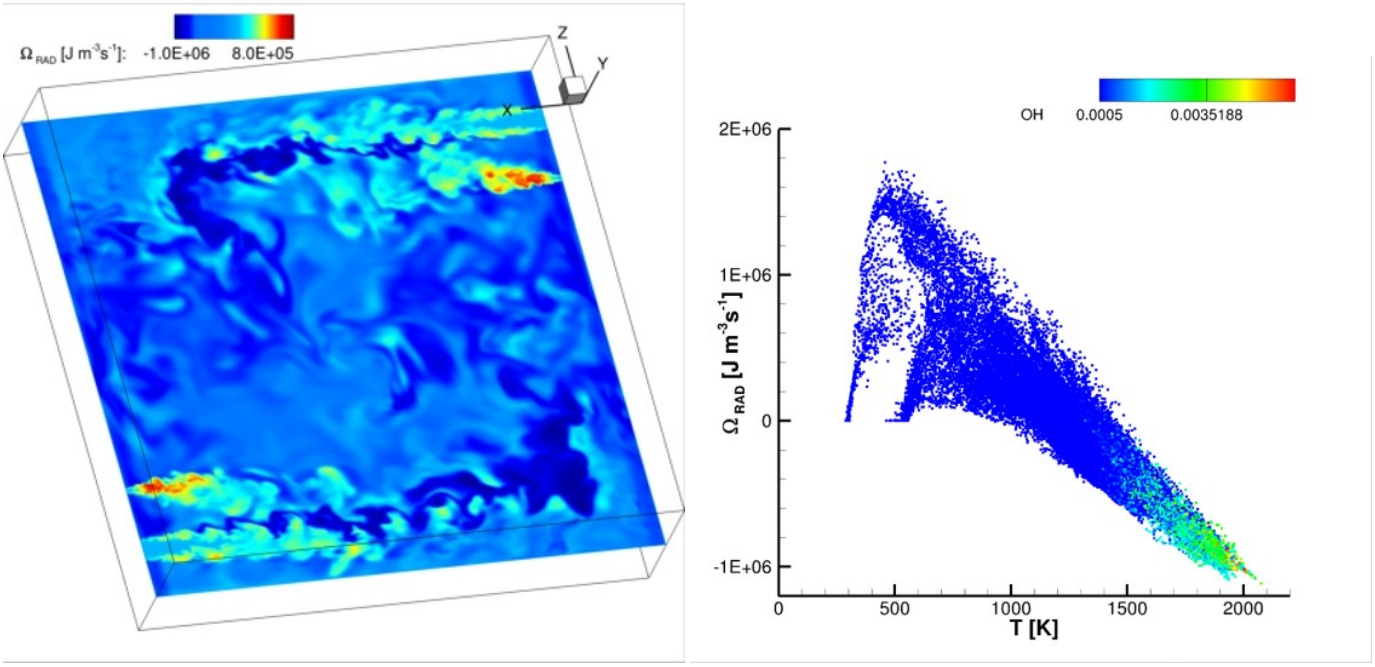

Figure 10. Instantaneous spatial distribution on a planar section of a cyclonic combustor burning hydrogen and air in non-premixed MILD combustion regime [69]. The distribution shown at the bottom is colored by means of the OH radical mass fraction.

When it comes to the peak flame temperature, radiation typically reduces it in low-pressure flames. Although radiation effects become more pronounced with increasing pressure, primarily due to the heightened emission and absorption of energy, the peak flame temperature is less affected by radiation. This is attributed to the faster chemical reactions that occur at higher pressures, a phenomenon also observed in [58] (p. 139). In fact, based on the Arrhenius law, the chemical reaction rate is directly proportional to the molar concentrations of the reactants raised to a power that corresponds to the number

of moles required to collide for the reaction to take place. As a result, the reaction rate is directly proportional to pressure (p) for first-order reactions and to the square of pressure (p^2) for second-order reactions. Three-body reactions are even more greatly influenced by pressure, as indicated in [71].

It is known that hydrogen flames have a lower emissivity than natural gas flames. Such radiative emission changes may have important implications in some applications [72].

In [39], a series of premixed Bunsen flames at a constant thermal power of 7.1 kW, burning methane and hydrogen in air at atmospheric pressure with increasing hydrogen content, were experimentally investigated. While increasing the hydrogen content, the thermal power was kept constant, maintaining the same laminar flame speed of the fuel mixture (hence, decreasing its equivalence ratio) and increasing the flow rate (hence, the jet Reynolds number). The spectrum of the electromagnetic radiation emitted was measured in a range of wavelengths between 200 and 1080 nm (nanometer), from ultraviolet to near infrared. The radiation emitted was collected by a system of lenses capable of focusing the image of the flame in an area of about 1–2 cm, where it was collected by an integrating sphere and sent, through an optical fiber, to a digital spectrometer. The integrating sphere is a spherical device which has the ability to concentrate almost all of the radiation collected inside it through a hole of about 1 cm made on its surface: measurement details can be found in [39,73]. The result is that, by integrating the measurement over a rather large surface of flame, the spatial dependence of the measurement is substantially lost, highlighting the spectral dependence on the wavelengths and the type of mixture.

Figure 11 shows the spectra of radiant energy emitted by flames in [39] with increasing hydrogen contents. The arrow with X_{H_2} defines the direction in which the molar fraction of hydrogen in the methane/air mixture increases. It starts from a pure methane flame, up to a pure hydrogen flame. The figure also shows the spectral emission lines of the major emitting species. As the carbon content in the mixture decreases, the decrease in energy emitted by the species CH, CO_2, C_2, H_2O, and H_2 is evident.

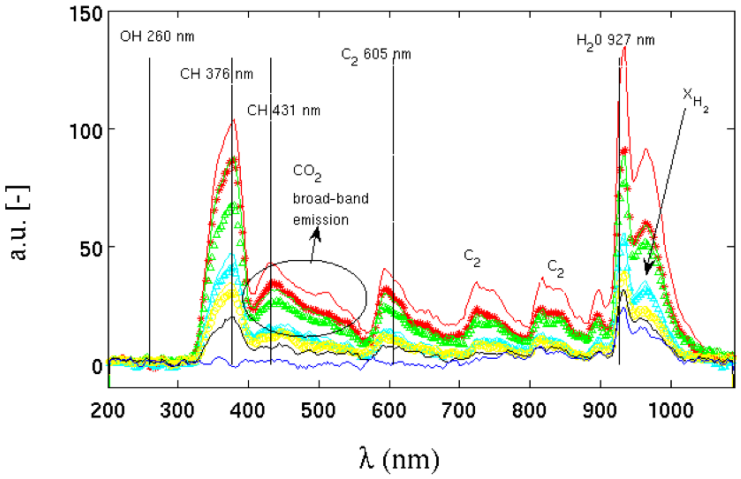

Figure 11. Emission spectrum at different hydrogen contents in the premixed CH_4/H_2/Air Bunsen flames studied in [39]. The X_{H_2} (hydrogen the molar fraction) arrow points to the increasing direction of the hydrogen molar fraction.

As the hydrogen content in the mixture increases, the contribution of carbon to the emission of radiative energy progressively decreases until, in the mixture of pure hydrogen, only the emission peak of water and H_2 survives, strongly reducing the ratio between radiant/convective energy emitted. In all mixtures, the emission peak of the OH radical, located in the ultraviolet around a wavelength between about 260 and 310 nm, is substantially absent, despite being a chemical species strongly present inside the flame front. According to the authors in [39], the reason for this absence could lie in the low sensitivity of the instrument at those wavelengths, such as to return a signal-to-noise ratio that is too

low for this type of measurement. Even with this lack, the differences in radiant energy emitted with the presence or absence of methane are considerable.

A lower radiative emission translates into a greater quantity of energy which is transmitted by convection, which mainly follows an axial direction, whereas the radiative one is emitted in all directions, and, given the cylindrical symmetry of the flame, preferentially in a radial direction. While this is beneficial for gas turbine applications (lower heat losses to walls and less cooling issues), it could be a serious issue in other industrial applications such as raw-material melting kilns or product cooking kilns.

In the same experiments [39], the temperature of a strongly absorbing metal body (black colored) positioned on the flame side at a distance of about 2 diameters D (D, the diameter of the Bunsen burner adopted) was measured by a thermocouple. The correlation between the radiant energy emitted in the radial direction and temperature is shown in Figure 12. It can be seen that, as the hydrogen content increases, the value of the integral of the radiative emission (I) is linearly anti-correlated with the temperature reached by the absorbent body. It can be deduced that the reduction in the chemical species that emit by chemiluminescence strongly influences the amount of radiative thermal energy emitted. It is also observed that up to a hydrogen volume content of 78% (30% by mass of hydrogen), this phenomenon is strongly limited: even a minimal quantity (in volume) of methane is sufficient to "color" the flame, which emits over a more extensive range of wavelengths; the flame is instead almost colorless when the carbon is absent.

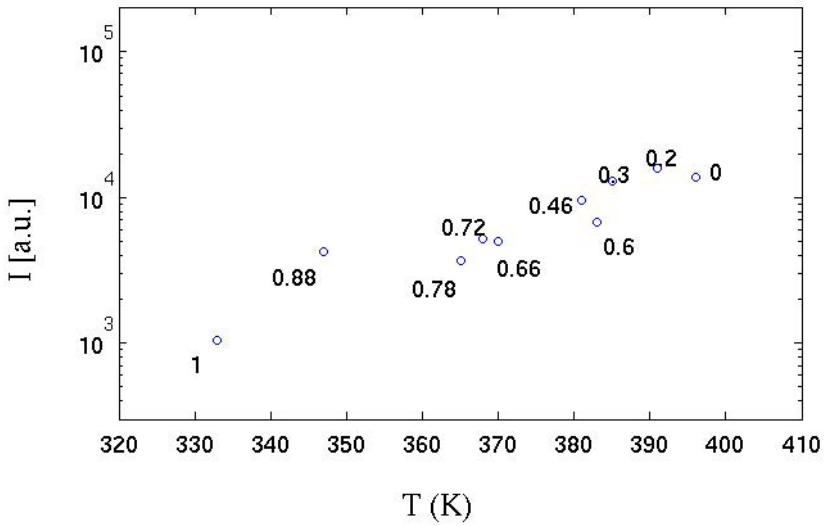

Figure 12. Integrated emission spectrum (over all wavelengths) for the various hydrogen contents vs. the temperature measured in the radial direction for the premixed $CH_4/H_2/Air$ Bunsen flames studied in [39]. Each experimental point is labeled with molar fraction of hydrogen. See Figure 1 for the equivalence between hydrogen mass and volume fraction.

2.4. Effects on Materials

Besides affecting combustion characteristics, hydrogen enrichment to natural gas also affects materials. Hydrogen can be absorbed by certain containment materials and piping, potentially leading to the loss of ductility or embrittlement in them. Hydrogen embrittlement becomes evident shortly after its introduction into a system and is an irreversible process. This phenomenon diminishes the material's yield stress, consequently compromising its fatigue resilience, particularly under low-cycle fatigue conditions [74]. The extent and rapidity of embrittlement is accelerated by factors such as high temperature, pressure, and stress levels. It is important to note that not all materials exhibit the same susceptibility to hydrogen embrittlement. Stainless steels and nickel alloys, which are frequently employed in gas turbine combustion systems, are particularly prone to heightened embrittlement at elevated temperatures. This complicates the selection of materials for

combustion hardware, weld joints, and braze joints due to the need to mitigate the effects of hydrogen embrittlement.

A 100% hydrogen flame is typically shorter and positioned much closer to the burner when compared to a methane flame operating under the same conditions. This difference is primarily due to the higher flame speed and shorter ignition times associated with hydrogen, as highlighted in [37]. Conversely, industrial experience has shown that, when high percentages of water or steam are added to the fuel, the flame length can significantly increase. This, in combination with the elevation of flame temperature, carries important implications for the potential impact on combustor materials, as discussed in [75]. The most significant worry concerning hot gas path components arises from the fact that hydrogen's elevated combustion temperature leads to a rise in turbine firing temperature. Furthermore, the gas temperature profile upon leaving the combustor will be hotter and exhibit distinct characteristics when burning hydrogen in comparison to natural gas. This heightened firing temperature and alterations in the combustion profile shape will necessitate modifications in the designs of component cooling and coatings to avert any reduction in part lifespan.

It is also crucial to take into account that the combustion of hydrogen results in a change in the composition of the exhaust gases compared to the use of natural gas. This alteration in the composition of combustion products can have a notable impact in direct combustion equipment, particularly in situations where the combustion gases directly interact with the products being produced, as mentioned in [76,77]. In cases where direct-fired equipment mixes flue gases with significant amounts of fresh air before they come into contact with the product, such as in dryers operating at approximately 200 °C, this is less likely to be a major issue. However, further testing is advisable to confirm this. In contrast, in certain applications like glass kilns or lime kilns, where the flue gases are not mixed before they contact the product, changes in flue gas composition could potentially affect the quality of the product itself, for instance, by influencing the volatility of sulfate in glass furnaces, as discussed in [77]. A particular concern is the increased moisture content of flue gases [77] and the potential consequences this might have within furnaces and other direct-fired equipment, as highlighted in [72].

3. Gas Turbine and Piston Engines Power Generation

Although natural gas currently stands as the most environmentally friendly option among major combustion fuels, employing it contributes to roughly 20% of the total CO_2 emissions, with nearly 15% for power generation in the United States [78]. Hydrogen is a viable fuel option for both reciprocating gas engines and gas turbines to reduce CO_2 emissions, but its use in power generation is negligible at present, accounting for less than 0.2% of the electricity supply [1].

3.1. Hydrogen Piston Engines

Hydrogen can be effectively employed in piston engines when blended with hydrocarbons, utilizing fuel and injection systems similar to conventional gasoline engines. Consequently, hydrogen-powered vehicles represent a promising way to diminish the reliance on fossil fuels within the automotive sector; a history of hydrogen combustion vehicles can be found in [79].

Some of the already mentioned properties of hydrogen in Section 2 can have a positive impact on the use of H_2 as fuel in piston engines: its wider flammability range; its very low ignition energy (an order of magnitude less than gasoline); its high octane number (due to the self-ignition temperature being higher than gasoline), above 130, offering a high resistance to knocking combustion [80]; its high diffusivity, facilitating the formation of uniform fuel–air mixtures; its high flame speed (an order of magnitude higher than gasoline); and injected in a gaseous state, it provides optimal cold start performance. Some other features can have negative impacts: since the quenching distance is smaller than that of gasoline, the flame can propagate closer to the cylinder, causing serious flashback problems when reaching the inlet valve; due to the very low density of hydrogen, storage

tanks can result in volume problems, and the energy density of the air/hydrogen mixture and, therefore, the power is reduced.

Using hydrogen as a fuel in piston engines requires significant engine modifications, particularly in the areas of fuel–air mixture injection, compression, and ignition.

The mode of injection plays a crucial role in influencing airflow distribution, impacting the mixing and combustion of hydrogen and air. For hydrogen, direct high-pressure or low-pressure injection (depending on the phase of the cycle) is considered the optimal choice [80–82]. This method involves injecting fuel with the intake valve closed, reducing the risk of premature mixture ignition and preventing backfires in the delivery channel. However, injecting hydrogen into the intake port can lead to airflow blockage, potentially decreasing engine power and even causing engine shutdown, especially when higher hydrogen levels are required for increased power. Attempts to enhance power through supercharging introduce challenges such as increased risk of hot spot formation, backfires, and pre-ignition, which require leaner fuel ratios, limiting potential power gains.

Achieving the highest efficiency with hydrogen in piston engines might necessitate a higher compression ratio compared to gasoline engines [83]. This is because the self-ignition temperature of hydrogen is higher. The temperature increase during compression is directly linked to the compression ratio, so a higher self-ignition temperature permits a higher compression ratio, and this, in turns, improves efficiency.

Regarding spark plugs, they must prevent the electrode temperature from exceeding the ignition threshold and causing backfires. It is worth noting that platinum electrode spark plugs are not suitable for hydrogen use [83], as their catalytic properties could encourage hydrogen oxidation.

Direct injection [82] prevents flame propagation within the intake circuit but may not necessarily prevent pre-ignition inside the combustion chamber. To address pre-ignition issues, techniques like exhaust gas recirculation (EGR) are employed to introduce thermal dilution [84]. EGR helps lower the temperature of hot spots, reducing the chances of pre-ignition. Additionally, this method decreases combustion temperature peaks, leading to a reduction in NO_x emissions.

Compared to gasoline vehicles, hydrogen-powered vehicles can produce equivalent or even up to 20% higher levels of NO_x emissions. However, the use of a selective catalytic reduction (SCR) system can effectively reduce NO_x by catalytically decreasing nitrogen oxides in the exhaust gas, employing ammonia as a reducing agent.

Although the most advanced gas-reciprocating (or piston) internal combustion engines are capable of accommodating gases containing hydrogen content of up to 70% on a volumetric basis [85] and several manufacturers have showcased the feasibility of engines that operate using 100% hydrogen (anticipated to become commercially accessible in the near future), they can be generally fed with a fraction of about 30%, going beyond 50% by adjusting the compression and power in some cases. The main problems are the increased explosion limits and tendency to detonate, and the increased size of the fuel injection system, which can lead to a downgrading of engine displacement by more than 30%. Other issues include increased NO_x emissions. This may require the installation of catalytic exhaust systems, which are already used in some gas engines.

The major manufacturers of hydrogen piston engine vehicles include brands such as: Ford, BMW, Mazda, Chevrolet and Toyota. The characteristics of these engines can be found in [79]. Just as an example, Figure 13 reports Mazda's RX-8 Hydrogen RE, an intriguing solution featuring a hydrogen Wankel rotary engine [86]. This engine is supplied with hydrogen gas through an electronically controlled direct injection system. The use of a Wankel rotary engine offers a notable advantage in this context. This engine design employs separate chambers for induction and combustion, which helps mitigate the issue of backfiring commonly encountered when using hydrogen in piston engines.

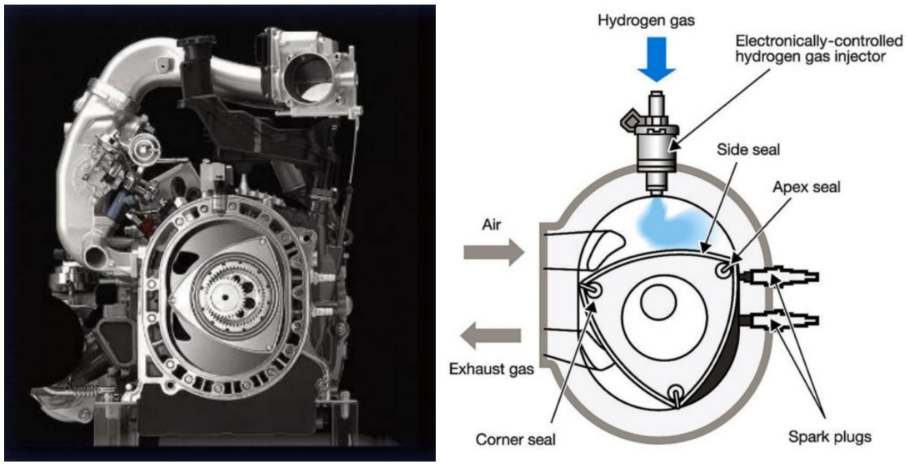

Figure 13. Mazda's RX-8 Hydrogen RE hydrogen Wankel rotary engine [79,86].

3.2. Hydrogen Gas Turbines

Thermo-electric power generation with gas turbines is one of the most immediately applicable solutions for reducing CO_2 emissions. However, a significant share of CO_2 emissions in the power generation sector can be attributed to gas turbines: utilizing hydrogen combined with natural gas will progressively become more significant in the effort to decrease CO_2 emissions. While renewable energy sources are making progress on the global energy stage, gas turbines will maintain their prominence in power generation both during the energy transition period and in the future energy scenario with an increasing percentage of non-programmable renewable sources, thanks to their capability to provide flexibility to the electric grid system [87,88]. In this vision, it has to be accepted that, over the years, the very concept of the gas turbine will undergo a natural evolution, adapting to the technological advances offered by the market. The flexibility of gas turbines gathers both their "load-flexibility" or "operational flexibility", and their "fuel-flexibility" [89]. Load flexibility, in the context of gas turbines, pertains to the turbine's ability to swiftly adjust its power output, contributing to the rapid stabilization of the electric grid. Various solutions have been suggested and put into practice in recent years, as noted in [90–92]. These efforts have resulted in the achievement of a power ramp rate of 10% of the nominal power per minute, which appears to be satisfactory for gas turbine users at present. This capability should be maintained as we transition to hydrogen gas turbines in the future. Fuel flexibility, on the other hand, relates to a gas turbine's capacity to operate effectively with various types of fuels, and more specifically for the present time, with fuel blends with a varying hydrogen content [93]. However, despite the considerable efforts and investments made by various manufacturers in recent years, the actual fuel-flexibility of the machines, i.e., their stable, efficient, clean, reliable, and safe operation from 100% natural gas to 100% hydrogen with varying hydrogen content, is a challenge yet to be overcome due to technological issues in the combustion system.

Hydrogen significantly modifies the combustion characteristics of a reacting mixture in comparison to natural gas. Specifically, the following changes are observed: a decrease in the ignition delay time; the enlargement of flammability limits; an increase in laminar flame speed; an increase in turbulent flame speed, which also becomes more pressure-dependent [94,95]; an increase in the adiabatic flame temperature. Hence, apart from issues related to its production, storage (lower vapor density), and transportation, safety issues also arise from such changes. In particular, the broader flammability range amplifies the potential for fuel ignition within the mixing passages; combustion dynamics can be dramatically affected by dangerous flashbacks due to the increased flame speed [96] and/or thermo-acoustic instabilities [97,98] that can lead to unexpected maintenance interventions, consequently diminishing the overall system's reliability. Despite extensive research and industrial efforts over the years, the issue of combustion instability remains partially

unresolved. The strategies typically employed to mitigate the potentially hazardous consequences of these instabilities in modern gas turbines primarily rely on empirical methods. Furthermore, the impact of hydrogen content on combustion dynamics has raised concerns about the reliability of the Wobbe index as a measure of fuel interchangeability, as discussed in [99]. During transient operations, such as start-up and shutdown, these dynamics become a primary concern. The implementation of advanced sensors for real-time combustion monitoring can be a key requirement [100,101]. For the foreseeable future, the inclusion of a safe fuel like natural gas will remain necessary for non-steady operations such as startup, shutdown, and part-load scenarios. Startup procedures typically rely on natural gas or liquid fuels, often involving a combination of diffusive and premixed combustion, at least up to the full-speed no load (FSNL) condition. Currently, it is generally acceptable to include an average volume that is 5% hydrogen during the startup phase. In essence, the stable operability window for many lean premixed combustors becomes narrower due to these dynamics.

Controlling temperature peaks to restrict NO_x emissions requires special consideration. Keeping these peaks below the existing natural gas limits of 25 parts per million by volume (ppmv) seems to be a challenging endeavor for gas turbines operating within the 0–100% hydrogen range until 2030. Achieving this goal is difficult because higher temperatures can be easily reached in the process. It has been observed that hydrogen changes the exhaust gas composition (more water) and that the gas turbine power should also be considered. For these reasons, there is an open discussion in gas turbine associations and OEMs about how to take into account such operating conditions in the law limits: a very promising suggestion to discuss with regulatory entities is to quantify such emissions as the ratio between the mass of NO_x at the exit and the input fuel energy (mg/MJ) [102].

Burning fuel mixtures with a high hydrogen content also has another significant impact—an increase in the steam content within the exhaust gases. This, in turn, leads to heightened heat exchange in the hot section of the gas turbine, necessitating additional cooling, as mentioned in [103]. However, this increased exposure to steam also raises concerns about hot corrosion and shortens component lifecycles. To address these challenges, a commonly adopted solution is to reduce the turbine inlet temperature, which results in a reduction in the machine's power output. While this approach can help mitigate the risk of hot corrosion, it comes at the cost of a 2% point reduction in efficiency, making it another challenging aspect to maintain until 2030, as discussed in [104].

Furthermore, for a fixed heat release, using a blend with 100% hydrogen necessitates an extra volumetric flow of fuel, approximately three times more than that needed for methane, making the direct and seamless utilization of hydrogen in gas turbines challenging.

In the end, necessary modifications in design are highly contingent on the proportion of hydrogen intended for combustion. The utilization of hydrogen can be categorized into groups based on the volume percentage: low (5–10%), medium (10–50%), and high (more than 50%) blends. Turbines operating with a low hydrogen blend may not necessitate design alterations, as the fuel-burning characteristics closely resemble those of a pure natural gas stream. In the case of medium blends, the overall architecture and combustor of the turbine might remain largely unchanged, but adjustments to combustor materials, fuel nozzles, and control systems will be essential. The development of retrofit solutions for existing gas turbines is certainly a key factor. When dealing with higher hydrogen blends exceeding 50%, extensive modifications to the turbines become imperative, and a comprehensive retrofit of the combustion system is likely required. Numerous original equipment manufacturers (OEMs) are presently engaged in developing new combustion systems capable of accommodating elevated hydrogen blend levels.

Hence, as the proportion of hydrogen in the fuel increases, an unmodified combustion system encounters greater challenges. Compounding these difficulties, in the foreseeable future, combustion systems will need to retain both fuel flexibility and the capability to burn natural gas.

While research is very advanced for low levels of hydrogen, it is significantly less so for high levels. The state of the art on hydrogen combustion is based on two combustion modes: diffusion flames with nitrogen, water or steam as diluent and lean premixed flames.

In combustion systems utilizing a diffusion flame and the addition of diluents, it is feasible to accommodate up to 100% volume of hydrogen. Nevertheless, such systems come with several drawbacks. These include reduced efficiency when compared to systems that do not use dilution, elevated levels of nitrogen oxides (NO_x) in comparison to lean premix technology, increased plant complexity, and consequently higher construction and maintenance costs.

Dry premixed combustion technology (dry low-emission, DLE, or dry low NO_x, DLN) does not implement any dilution; it is typically lean premixed or partially premixed to enable the better control of temperature and NO_x emissions. Effective mixing is essential for the abatement process. However, achieving the right residence times and sufficient volumes can be challenging to prevent self-ignition or flashback. In the lean premixed combustion, fuel and hot air mix in the mixing area but do not react until they enter the combustion chamber. It is important to note that these combustion strategies are prone to dangerous thermo-acoustic instabilities, especially near lean quench conditions. DLN/DLE combustion technologies can be categorized into four groups based on the approach used to stabilize combustion: combustion aerodynamically stabilized by propagation; combustion stabilized by self-ignition; staged combustion, stabilized using various methods (including propagation and self-ignition); micro-mixing combustion, involving multiple small flames that can be premixed, partially premixed, or diffusive. A comprehensive review of DLE gas turbine combustion technologies for hydrogen blends can be found in [69].

DLN/DLE combustion technology has greater potential than non-premixed and diluted combustion, but is not yet mature enough for very high hydrogen contents or when the greater flexibility of the fuel mix is required (e.g., to use natural gas/hydrogen mixtures with an H_2 content of 0–100%). The maximum permissible hydrogen concentration varies widely between manufacturers. Table 1 shows the levels of hydrogen currently accepted by the different classes of gas turbines [105,106], from heavy-duty, to industrial, to aeroderivative and microturbines (20% vol. H_2 refers to the lowest powers). The rationale behind these variations lies in the differences in combustion temperatures and the technologies employed within these distinct classes of gas turbines. When it comes to micro-gas turbines, despite the endeavors of certain original equipment manufacturers (OEMs), they do not progress along the learning curve at the same rate as their heavy-duty counterparts. This is mainly due to their limited tolerance for hydrogen. However, given that users of micro-gas turbines often rely on the same gas grid as larger turbines, it is essential to dedicate more efforts to research and development to attain a comparable level of hydrogen compliance.

Table 1. State of the art for gas turbines on the volume percentage accepted by the combustor [105].

Combustion	H_2% Vol.	NO_x | Complexity | CAPEX/OPEX
Non-premixed/diluted	0–100%	Higher
DLE lean premixed comb.	∼44–63% heavy duty (100–500 MWe) ∼43–55% industrial (30–100 MWe) ∼35% aeroderivative (1–30 MWe) ∼20–32% microturbine (0.1–1 MWe)	

Currently, there are no fuel-flexible DLE machines on the market capable of handling the entire 0–100% range of hydrogen mixed with natural gas. The technical experience accumulated with high hydrogen syngas (30 and 60% vol. of H_2 and CO), revisited and adapted, has proved useful. As a result, most gas turbine manufacturers offer units originally developed for syngas applications, which can also be used for natural gas/hydrogen mixtures with high H_2 levels (around 60% vol.). When examining the catalogs of OEMs, the current state-of-the-art in dry low emission (DLE) gas turbines reveals the capability to

burn hydrogen up to an average of 30% by volume while maintaining low NO_x emissions (below 25 ppmv at 15% oxygen). Due to the higher flame temperatures associated with hydrogen compared to natural gas, some cases control NO_x emissions solely by reducing the machine's power output, a practice known as derating, as discussed in [106]. It is worth noting that the strictest NO_x limits for natural gas (less than 15 ppmv at 15% oxygen) are not consistently met today. For instance, Ansaldo Energia GT36 and GT24/GT26 (as shown in Figure 14) gas turbines can accommodate up to 50% and 30% hydrogen by volume while still complying with the 15 ppmv limit, whereas AE94.3A and AE94.2 turbines can tolerate up to 25% hydrogen by volume while meeting the 25 ppmv compliance. As a result, a significant portion of investments are focused on DLE technology [69], specifically lean premixed combustion without dilution (e.g., steam, nitrogen, water), even for retrofit solutions. Moreover, new combustion concepts are being explored, including sequential combustion at constant pressure (as implemented in the GT36) [90,107], micro-mixing-based approaches [108], and exhaust gas recirculation (EGR) techniques [5,6].

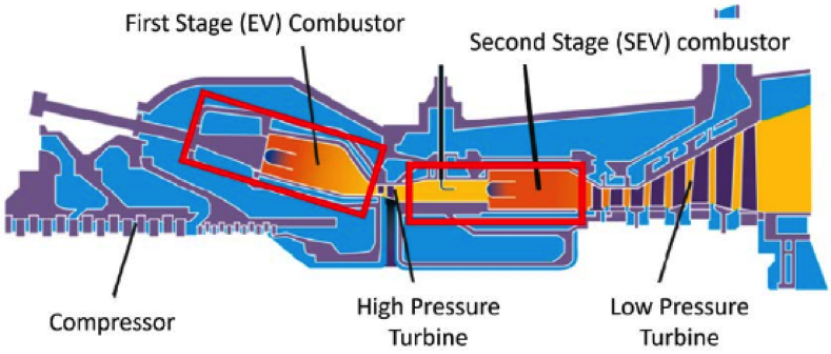

Figure 14. Section of the GT24/GT26 gas turbine illustrating the concept of sequential combustion [90].

Table 2 shows the key performance indicators (KPIs) for DLE gas turbines with reference to the state of the art (SoA) in 2020 and with forecasts to 2024 and 2030. It is noted that maintaining the same NO_x limits from 30 to 100% H_2 is already a challenge; moreover, the commonly adopted normalization for NO_x to 15% O_2 under dry conditions (without H_2O) cannot be applied to fuels with very different reactivity and combustion products than natural gas; a more appropriate normalization is that suggested in the same table, which uses the mass of NO_x in mg per quantity of fuel energy injected in MJ; this new normalization was suggested not only in the SRIA2021-2027 of the Clean Hydrogen Partnership [105], but also in the Hydrogen Working Group of the European Turbine Network [15]. As far as a start-up is concerned, it should be noted that this phase is typically carried out with only natural gas or liquid oil.

Table 2. Key performance indicators for DLE gas turbines [105]. NO_x refers to $NO + NO_2$. The maximum electrical efficiency loss refers to the full-speed full-load condition in combined cycle gas turbines. The minimum ramp rate is referred to the full-load condition.

KPI	Unit	SoA 2020	Target 2024	Target 2030
H_2 fuel content	% by mass % by volume	0–5 0–30	0–23 0–70	0–100 0–100
NO_x emissions	ppmv at 15%O_2 dry mmg/MJ_{fuel}	<25 at 30% vol. H_2 <31 at 30% vol. H_2	<25 at 70% vol. H_2 <29 at 70% vol. H_2	<25 at 100% vol. H_2 <24 at 100% vol. H_2
Max. H_2 content at start-up	% by mass % by volume	0.7 5	3 20	100 100
Max. electrical efficiency loss	% points	10 at 30% vol. H_2	10 at 70% vol. H_2	10 at 100% vol. H_2
Min. ramp rate	% load/minute	10 at 30% vol. H_2	10 at 70% vol. H_2	10 at 100% vol. H_2
H_2 accepted fluctuations	% by mass/minute % by volume/minute	±1.4 ±10	±2.21 ±15	±5.11 ±30

4. Hard-to-Abate Industry

Constituting 38% of the total final energy demand, the industrial sector stands as the most substantial end-use segment. Notably, this sector is responsible for 26% of the global energy system's CO_2 emissions [1]. Involving processes heavily relying on fossil fuels, the hard-to-abate sector is the most challenging in reducing pollutant emissions [72,109]: electrification is not a straightforward solution in most related industrial processes and the potential implementation of hydrogen opens some critical issues regarding the process itself and the quality of the product. Within the industrial landscape, hydrogen plays a role in utilizing 6% of the overall energy demand. This hydrogen is predominantly employed as feedstock in chemical production and as a reducing agent in the manufacturing of iron and steel. The annual industrial demand for hydrogen amounts to 51 million metric tons [1].

Table 3 reports combustion-based applications in the hard-to-abate sector.

Table 3. Combustion applications for the hard-to-abate sector, related processes, and equipments.

Applications	Processes	Equipments
Food	Hot water production, steam production, drying	Boiler, cogeneration, direct flame oven, dryer
Chemicals	Steam production, drying, cracking, direct heat at high temperature	Boiler, cogeneration, direct flame oven, dryer
Vehicle production	Varnishing, environmental heating, drying, hardening, welding, pressing	Boiler (also at high pressure), direct flame oven, dryer
Metals	Steel lamination and melting, melting of non-ferrous metals, thermal treatments	Various type of ovens
Refining	Distillation, reforming, isomerization, cracking, calcination, hydro-treatment, catalyzer regenaration, steam production	Oven, boiler, cogeneration
Paper	Hot water production, steam production, drying, refining, finishing	Boiler, cogeneration, direct flame dryer
Glass	Raw material melting, conditioning, annealing, molding, pressing	Gas oven for melting, annealing oven
Ceramic	Cooking of raw materials, drying, molding, finishing	Gas oven, dryer with recuperated heat, boiler for hot water
Cement	Cooking of raw materials	Lime kiln: regenerative (parallel fluxes) or vertical kilns (older)
Non-metallic minerals	Drying, melting, calcination, evaporation, separation	gas dryer, oven, boiler, CHP

Producers sell burners (generally working at atmospheric pressure) able to operate up to 100% H_2 usually in the chemical or refining sectors, where a subproduct of hydrogen is produced. Due to the high flame temperature, combustors' material have to be chosen suitably. In fact, the flame can easily attach close to the nozzles, making the choice of materials a serious concern. High-frequency noise can be avoided by means of silencers or damping devices. Some burners operating at 100% H_2 are non-premixed to reduce NO_x (for example, in the MILD or flameless combustion regime); others are DLE/DLN premixed. There exist burners without flashback up to 100% H_2.

Almost all glass is produced in furnaces where a mixture of raw materials is combined and melted into a homogeneous mixture. Like many industrial production processes, glass melting can be classified as a continuous or discontinuous (batch) process. The melting point of most glass is around 1400–1600 °C, depending on its composition. Consequently, glass production requires a large amount of thermal energy. Because of this high energy demand, glass furnaces are built to minimise heat loss and often feature some form of waste heat recovery system: regenerative, recuperative, electrical. The most commonly used fuels for glass melting furnaces are natural gas, light and heavy fuel oil, and liquefied petroleum gas. Methods are currently being investigated to increase the radiative qualities of hydrogen to make it a more viable alternative to natural gas. Traditionally, pure hydrogen has been considered unsuitable for glass melting. This is because the heat produced by its flame is

unable to penetrate the liquid glass bath well, leaving the top layer too hot and the bottom too cold. It has always been thought that a glass furnace requires a 'sooty' flame to function, as soot improves the radiant heat transfer. Moreover, existing hydrogen combustion systems have not proved suitable for rapid implementation in existing melting furnaces, as major changes in the composition of the furnace atmosphere are expected [72,77]. The influence of these variations on glass chemistry has not yet been adequately studied.

For the lime industry, in the most advanced dry process, raw materials are calcined at around 900–1250 °C in a pre-calciner to transform the limestone into lime, which releases CO_2 as a by-product. The materials are then fed into a rotary kiln, where they aggregate to form clinker at 1450 °C with flame temperatures reaching 2000 °C. The fuel can be coal gas or hydrogen-rich syngas. In the lime industry, the water content of the flue gas would pose a significant challenge [72]. Calcium oxide in fact reacts with steam, causing problems with the quality, efficiency, durability, and safety of the product.

Besides being used as a reducing agent, hydrogen has great potential as a fuel in the steel production process. The possible applications of hydrogen mainly concern the production of pellets, the sintering process, reheating, and heat treatment furnaces. Several manufacturers of combustion systems for the steel industry already market some MILD or flameless type furnaces, which have been successfully tested with a variety of mixtures of natural gas and hydrogen, up to 100% hydrogen. In the MILD combustion mode, the heat release is distributed over a large volume, ensuring an even heat distribution, which is very effective for the material being processed. Products available on the market include, for example, TENOVA's TSX series [110] of reheating furnaces with NO_x emissions below 80 mg/Nm^3 at 5% O_2, with a furnace temperature of 1250 °C; in 2022, TENOVA also built the first industrial furnace with TRKSX combustion systems [111] for heat treatment in MILD mode up to 100% hydrogen, with NO_x emissions compatible with future, more stringent regulatory limits. Among other applications, LINDE also invested in oxy-combustion, which can reduce both energy consumption and emissions [112]; in 2020, it tested a full-scale MILD oxy-combustion reheating furnace in Sweden with up to 100% hydrogen with its REBOX HyOx combustion system [113].

Roller kilns are commonly utilized in the ceramics industry because of their efficiency in achieving temperature variations. They achieve this by moving the product through zones of different temperatures along the length of the kiln, rather than periodically heating and cooling the entire kiln. Additionally, they enhance productivity by allowing for continuous production. In the ceramics industry, industrial kilns used for ceramic tile production are predominantly of the roller type, typically fueled by gas. These kilns can be quite extensive, reaching lengths of up to 300 m, and they may have several hundreds of burners positioned along their length. Depending on the specific type of production, these kilns must be capable of maintaining temperatures of up to 1250 °C, while it is preferable to keep the silicon carbide (SiC) burner tubes, which contain the flame, at temperatures below 1300 °C. Fuels can be natural gas, LPG, diesel, paraffin, and other liquid fuels up to temperatures of 1800 °C. In the case of hydrogen, the great challenge concerns the moisture content of the combustion gases, since the ultimate goal of ceramic production is to remove moisture [114].

The use of hydrogen in boilers [115] is common in those sectors where hydrogen is a waste product of chemical processes. Consequently, there are a number of known technological measures for its safe and efficient handling. This particularly concerns piping, nozzles, and high-temperature resistant components that come into contact with flames, burner fans, and the combustion chamber. A 100% hydrogen-fueled boiler can be up to 10% larger than a natural gas boiler producing the same output. Flue gas recirculation is generally used to lower the average flame temperature and contain NO_x. To prevent the ignition of the mixture in the supply line, the system is equipped with upstream flame breakers. In steam boilers [116], when switching from natural gas to hydrogen, the variation in heat absorption between the radiant/convective sections can be mitigated by regulating the feedwater split between the two sections.

Table 4 briefly compares the applications described above and the barriers/problems for using hydrogen in the device considered.

Table 4. Main applications of the hard-to-abate sector and barriers to hydrogen implementation.

Applications	Equipments	Temperature [°C]	Fuels	Hydrogen Barriers 5
Glass	Melting ovens	1400–1600	Natural gas, oil, LPG	Low radiation, unknown effects of the different combustion products emission
Lime	Rotary kilns	1450–2000	Coal gas, H_2-rich syngas	Higher H_2O content in combustion products
Steel	Ovens for heating and thermal treatments	800–1400	Natural gas, coal gas, syngas, LPG	No barriers, for both raw material and combustion emissions
Ceramic	Roller kilns	1250–1800	Natural gas, LPG, diesel, kerosene	Higher H_2O content in combustion products
Hot water, steam, drying	Boilers	1200–1400	Natural gas	Volumes higher than 10% for a certain power

5. Conclusions and Future Directions

Hydrogen introduces a remarkable potential for a substantial reduction in CO_2 emissions. Numerous technologies are currently in existence or in development, poised to facilitate the integration of hydrogen into the future energy landscape. While these technologies hold great promise, the primary hurdles lie in achieving the necessary scale and ensuring the economic viability and genuine environmental friendliness of hydrogen generation, distribution, and utilization.

In the present day, and it is presumed at least until 2030, the primary challenges in adopting hydrogen technology will not be technological but rather centered around hydrogen availability and cost. Currently, approximately 70 million tons of hydrogen are produced globally each year, with 99% of this production originating from coal and natural gas sources. However, if all hydrogen production were to transition to water electrolysis, it would require an estimated 3600 terawatt–hours (TWh) of electrical energy per year, which is more than the entire annual electricity production of the entire European Union, as noted by the International Energy Agency (IEA) in 2019 [117]. Availability issues become even more challenging if the electricity for water electrolysis is sourced from excess energy generated by variable renewable energy sources (VRESs). To put this into perspective, the amount of wind power generation curtailed in Germany in 2016 was 4722 gigawatt–hours (GWh), whereas the energy required to produce hydrogen through electrolysis to power just one General Electric 9HA.02 gas turbine for 8000 h at nominal power is 19,600 GWh, as outlined in the study by Goldmeer [85]. Therefore, even without considering the cost aspect, from this standpoint, the authors believe that the use of blue hydrogen, produced from fossil fuels with carbon capture and storage, will be essential to establish a practical hydrogen value chain. This approach can pave the way for the broader utilization of green hydrogen, produced through renewable energy sources, once it becomes available in sufficient quantities to effectively reduce carbon dioxide emissions.

In the power sector, gas turbines will persist as a crucial component within the global energy framework, as they complement renewable energy sources and possess a significant existing installed base. Gas turbines are called upon to serve as a backup (seasonal and peak), supporting variable renewable energy sources and maintaining the stability of the electric grid, including voltage and frequency control. This contribution to electric system flexibility is expected to be significant, even in a projection for the year 2040, as illustrated in Figure 15, which estimates that the annual operating hours will be less than 3000. In this context, post-combustion carbon capture technologies are deemed impractical, both from a technical and economic perspective, as indicated in a report by AECOM in 2020 [118]. It is

worth noting that the potential annual reduction in carbon dioxide emissions is achievable with 100% hydrogen gas turbines exceeding 450 million tons in this scenario.

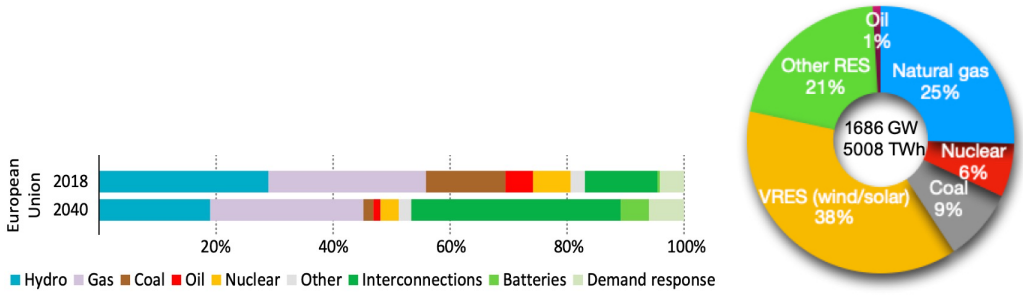

Figure 15. Capacity of the European electricity system under existing policies and sources of flexibility with stated policies in the projected 2040 scenario by the IEA [119].

Despite the long history of gas turbines and their diverse applications across various sectors, ongoing research and development efforts are necessary to ensure their reliable and safe operation with a higher hydrogen content. The aim is to reach a hydrogen content of at least 80% by volume, which can lead to a substantial reduction in CO_2 emissions. Original equipment manufacturers (OEMs) are dedicating substantial resources to incorporating hydrogen-burning technologies into their new engines and crafting modification packages for existing engines.

In the hard-to-abate sector, the reduction in pollutant emission is even more challenging. Electrification cannot be implemented in most industrial processes and hydrogen combustion cannot also be adopted in a straightforward way. In fact, substituting fuel blends with a high H_2 content for natural gas produces changes in the radiative energy emission and in exhaust gases composition that can have important effects on the industrial process and the quality of the products. Hence, some research is still needed and more importantly, communication between industries and research should be enhanced, especially in the glass and ceramic sectors. The application of hydrogen in furnaces for the steel industry is instead at an advanced stage.

Beyond the technological challenges that must be overcome, the most significant barrier to the widespread adoption of hydrogen is its availability, primarily due to its production cost. Once hydrogen is embraced as a key element in addressing climate change, the transition to a "hydrogen society" can only be realized by establishing the necessary infrastructure. In the authors' view, this transition should begin with the utilization of cost-effective "blue hydrogen" in the short term, followed by the integration of the more expensive "green hydrogen" in the long term.

Author Contributions: Structure, writing, E.G., G.T., A.D.N., G.C., D.C., G.M. and S.C.; sources, all; review, all. All authors have read and agreed to the published version of the manuscript.

Funding: This review study was performed within the Italian project "RICERCA E SVILUPPO DI TECNOLOGIE PER LA FILIERA DELL'IDROGENO POR-H2" ("Research and Development of Technologies for Hydrogen Chain", POR-H2, WP2, LA2.2.5), funded by the Italian Ministry of Environment and Energy Security, under the National Recovery and Resilience Plan (PNRR, Mission 2, Component 2, Investment 3.5, project code I83C22001170006).

Data Availability Statement: Data related to pictures where ENEA's articles or technical reports are cited can be directly asked to the corresponding author.

Conflicts of Interest: The authors declare no conflict of interest.

References

1. International Energy Agency. *Global Hydrogen Review*; Technical Report; IEA: Paris, France, 2021.
2. International Energy Agency. *Net Zero by 2050—A Roadmap for the Global Energy Sector*; Flagship Report; IEA: Paris, France, 2021.
3. Gubbi, S.; Cole, R.; Emerson, B.; Noble, D.; Steele, R.; Sun, W.; Lieuwen, T. Air Quality Implications of Using Ammonia as a Renewable Fuel: How Low Can NOx Emissions Go? *ACS Energy Lett.* **2023**, *8*, 4421–4426. [CrossRef] [PubMed]

4. Tanaka, Y.; Nakao, M.; Ito, E.; Nose, M.; Saitoh, K.; Tsukagoshi, K. *Development of Low NOx Combustion System with EGR for 780–1700 °C-Class Gas Turbine*; Technical Review 1; MITSUBISHI-HITACHI Heavy Industries: Tokyo, Japan, 2013.
5. Ditaranto, M.; Li, H.L.; Lovas, T. Concept of hydrogen fired gas turbine cycle with exhaust gas recirculation: Assessment of combustion 802 and emissions performance. *Int. J. Greenh. Gas Control* **2015**, *37*, 377–383. [CrossRef]
6. Ditaranto, M.; Heggset, T.; Berstad, D. Concept of hydrogen fired gas turbine cycle with exhaust gas recirculation: Assessment of 804 process performance. *Energy* **2020**, *192*, 116646. [CrossRef]
7. Panigrahy, S.; Mohamed, A.; Wang, P.; Bourque, G.; Curran, H. When hydrogen is slower than methane to ignite. *Proc. Combust. Inst.* **2023**, *39*, 253–263. [CrossRef]
8. Safta, C.; Madnia, C. Autoignition and structure of nonpremixed CH_4/H_2 flames: Detailed and reduced kinetic models. *Combust. Flame* **2006**, *144*, 64–73. [CrossRef]
9. Gersen, S.; Anikin, N.B.; Mokhov, H.B. Ignition Properties of Methane/Hydrogen Mixtures in a Rapid Compression Machine. *Int. J. Hydrogen Energy* **2008**, *33*, 1957–1964. [CrossRef]
10. Donohoe, N.; Heufer, A.; Metcalfe, W.K.; Curran, H.J.; Davis, M.L.; Mathieu, O.; Plichta, D.; Morones, A.; Petersen, E.L.; Güthe, F. Ignition delay times, laminar flame speeds, and mechanism validation for natural gas/hydrogen blends at elevated pressures. *Combust. Flame* **2014**, *161*, 1432–1443. [CrossRef]
11. Park, S. Hydrogen addition effect on NO formation in methane/air lean-premixed flames at elevated pressure. *Int. J. Hydrogen Energy* **2021**, *46*, 25712–25725. [CrossRef]
12. Sankaran, R.; Im, H.R. Effects of Hydrogen Addition on the Markstein Length and Flammability Limit of Stretched Methane/Air Premixed Flames. *Combust. Sci. Technol.* **2006**, *178*, 1585–1611. [CrossRef]
13. Imteyaz, B.A.; Nemitallah, M.A.; Abdelhafez, A.A.; Habib, M.A. Combustion Behavior and Stability Map of Hydrogen-Enriched Oxy-Methane Premixed Flames in a Model Gas Turbine Combustor. *Int. J. Hydrogen Energy* **2018**, *43*, 16652–16666. [CrossRef]
14. Nemitallah, M.A.; Imteyaz, B.; Abdelhafez, A.; Habib, M.A. Experimental and Computational Study on Stability Characteristics of Hydrogen-Enriched Oxy-Methane Premixed Flames. *Appl. Energy* **2019**, *250*, 433–443. [CrossRef]
15. ETN Global. *Addressing the Combustion Challenges of Hydrogen Addition to Natural Gas*; ETN Position Paper; European Turbine Network: Brussels, Belgium, 2022.
16. Boschek, E.; Griebel, P.; Jansohn, P. Fuel Variability Effects on Turbulent, Lean Premixed Flames at High Pressures. In Proceedings of the GT2007, ASME Turbo Expo 2007: Power for Land, Sea and Air, Montreal, QC, Canada, 14–17 May 2007; ASME: New York, NY, USA, 2007; number GT2007-27496.
17. Huang, Z.; Zhang, Y.; Zeng, K.; Liu, B.; Wang, Q.; Jiang, D. Measurements of laminar burning velocities for natural gas–hydrogen–air mixtures. *Combust. Flame* **2006**, *146*, 302–311. [CrossRef]
18. Hu, E.; Huang, Z.; He, J.; Jin, C.; Zheng, J. Experimental and numerical study on laminar burning characteristics of premixed methane–hydrogen–air flames. *Int. J. Hydrogen Energy* **2009**, *34*, 4876–4888. [CrossRef]
19. Zhang, W.; Wang, J.; Lin, W.; Li, G.; Hu, Z.; Zhang, M.; Huang, Z. Effect of hydrogen enrichment on flame broadening of turbulent premixed flames in thin reaction regime. *Int. J. Hydrogen Energy* **2021**, *46*, 1210–1218. [CrossRef]
20. Schefer, R.W.; Wicksall, D.; Agrawal, A.K. Combustion of hydrogen-enriched methane in a lean premixed swirl-stabilized burner. *Proc. Combust. Inst.* **2002**, *29*, 843–851. [CrossRef]
21. Cicoria, D.; Chan, C. Effects of turbulence and strain rate on hydrogen-enriched high Karlovitz number lean premixed methane flames. *Fuel* **2018**, *211*, 754–766. [CrossRef]
22. Mashruk, S. Nitric Oxide Formation Analysis Using Chemical Reactor Modelling and Laser Induced Fluorescence Measurements on Industrial Swirl Flames. Ph.D. Thesis, School of Engineering, Cardiff University, Cardiff, UK, 2020.
23. Lavadera, M.; Brackmann, C.; Konnov, A. Experimental and modeling study of laminar burning velocities and nitric oxide formation in premixed ethylene/air flames. *Proc. Combust. Inst.* **2021**, *38*, 395–404. [CrossRef]
24. Konnov, A.A. Yet another kinetic mechanism for hydrogen combustion. *Combust. Flame* **2019**, *203*, 14–22. [CrossRef]
25. Glarborg, P.; Miller, J.; Ruscic, B.; Klippenstein, S. Modeling nitrogen chemistry in combustion. *Prog. Eneegy Combust. Sci.* **2018**, *67*, 31–68. [CrossRef]
26. Song, Y.; Marrodán, L.; Vin, N.; Herbinet, O.; Assaf, E.; Fittchen, C.; Stagni, A.; Faravelli, T.; Alzueta, M.; Battin-Leclerc, F. The sensitizing effects of NO_2 and NO on methane low temperature oxidation in a jet stirred reactor. *Proc. Combust. Inst.* **2019**, *37*, 667–675. [CrossRef]
27. Metcalfe, W.; Burke, S.; Ahmed, S.; Curran, H. A Hierarchical and Comparative Kinetic Modeling Study of C1-C2 Hydrocarbon and Oxygenated Fuels. *Int. J. Chem. Kinet.* **2013**, *45*, 638–675. [CrossRef]
28. Lieuwen, T.; McDonell, V.; Petersen, E.; Santavicca, D. Fuel flexibility influences on premixed combustor blowout, flashback, autoignition, and stability. *J. Eng. Gas Turbines Power* **2008**, *130*, 011506. [CrossRef]
29. Matalon, M.; Matkowsky, B.J. Flames as gasdynamic discontinuities. *J. Fluid Mech.* **1982**, *124*, 239–259. [CrossRef]
30. Clavin, P.; Williams, F. Effects of molecular diffusion and of thermal expansion on the structure and dynamics of premixed flames in turbulent flows of large scale and low intensity. *J. Fluid Mech.* **1982**, *116*, 251–282. [CrossRef]
31. Sivashinsky, G. Nonlinear analysis of hydrodynamic instability in laminar flames—I. Derivation of basic equations. *Acta Astronaut.* **1977**, *4*, 1177–1206. [CrossRef]
32. Law, C.K.; Jomaas, G.; Bechtold, J.K. Cellular instabilities of expanding hydrogen/propane spherical flames at elevated pressures: Theory and experiment. *Proc. Combust. Inst.* **2005**, *30*, 159–167. [CrossRef]

33. Liu, Z.; Yang, S.; Law, C.K.; Saha, A. Cellular instability in Le < 1 turbulent expanding flames. *Proc. Combust. Inst.* **2019**, *37*, 2611–2618.
34. Creta, F.; Lapenna, P.E.; Lamioni, R.; Fogla, N.; Matalon, M. Propagation of premixed flames in the presence of Darrieus–Landau and thermal diffusive instabilities. *Combust. Flame* **2020**, *216*, 256–270. [CrossRef]
35. Rocco, G.; Battista, F.; Picano, F.; Troiani, G.; Casciola, C.M. Curvature effects in turbulent premixed flames of H 2/air: A DNS study with reduced chemistry. *Flow Turbul. Combust.* **2015**, *94*, 359–379. [CrossRef]
36. Berger, L.; Attili, A.; Pitsch, H. Synergistic interactions of thermodiffusive instabilities and turbulence in lean hydrogen flames. *Combust. Flame* **2022**, *244*, 112254. [CrossRef]
37. Cecere, D.; Giacomazzi, E.; Picchia, F.R.; Arcidiacono, N.M. Direct Numerical Simulation of a Turbulent Lean Premixed CH_4/H_2-Air Slot Flames. *Combust. Flame* **2016**, *165*, 384–401. [CrossRef]
38. Troiani, G.; Lapenna, P.E.; Alessio, F.D.; Creta, F. Experimental dataset of H_2/CH_4-air Bunsen flames: Interplay of intrinsic instabilities and turbulence. In Proceedings of the 11th European Combustion Meeting, Rouen, France, 26–28 April 2023; pp. 1320–1325.
39. Troiani, G.; Giacomazzi, E.; Marrocco, M.; Di Nardo, A.; Scaccia, S.; Calchetti, G.; Cecere, D.; Assettati, A.; Guidarelli, G.; Stringola, C.; et al. *La Combustione di Idrogeno nella Transizione Energetica e Sperimentazione Atmosferica di un Bruciatore con Miscele Metano/Idrogeno in Aria*; Technical Report D2.2.5.2 of POR-H2 Project; ENEA, Casaccia Research Centre: Rome, Italy, 2023.
40. Bechtold, J.; Matalon, M. The dependence of the Markstein length on stoichiometry. *Combust. Flame* **2001**, *127*, 1906–1913. [CrossRef]
41. Troiani, G.; Creta, F.; Matalon, M. Experimental investigation of Darrieus–Landau instability effects on turbulent premixed flames. *Proc. Combust. Inst.* **2015**, *35*, 1451–1459. [CrossRef]
42. Creta, F.; Lamioni, R.; Lapenna, P.E.; Troiani, G. Interplay of Darrieus-Landau instability and weak turbulence in premixed flame propagation. *Phys. Rev. E* **2016**, *94*, 053102. [CrossRef]
43. Lapenna, P.E.; Troiani, G.; Lamioni, R.; Creta, F. Mitigation of Darrieus–Landau instability effects on turbulent premixed flames. *Proc. Combust. Inst.* **2021**, *38*, 2885–2892. [CrossRef]
44. Troiani, G.; Lapenna, P.; Lamioni, R.; Creta, F. Self-wrinkling induced by Darrieus-Landau instability in turbulent premixed Bunsen flames from low to moderately high Reynolds numbers. *Phys. Rev. Fluids* **2022**, *7*, 053202. [CrossRef]
45. Lamioni, R.; Lapenna, P.E.; Troiani, G.; Creta, F. Strain rates, flow patterns and flame surface densities in hydrodynamically unstable, weakly turbulent premixed flames. *Proc. Combust. Inst.* **2019**, *37*, 1815–1822. [CrossRef]
46. Brower, M.; Petersen, E.; Metcalfe, W.; Curran, H.J.; Furi, M.; Bourque, G.; Aluri, N.; Guthe, F. Ignition Delay Time and Laminar Flame Speed Calculations or Natural Gas/Hydrogen Blends at Elevated Pressures. *J. Eng. Gas Turbines Power* **2012**, *135*, 021504. [CrossRef]
47. Ebi, D.; Jansohn, P. Boundary Layer Flashback Limits of Hydrogen-Methane-Air Flames in a Generic Swirl Burner at Gas Turbine Relevant Conditions. In Proceedings of the ASME Turbo Expo 2020, Turbomachinery Technical Conference and Exposition, London, UK, 22–26 June 2020.
48. Beita, J.; Talibi, M.; Sadasivuni, S.; Balach, R. Thermoacoustic Instability Considerations for High Hydrogen Combustion in Lean Premixed Gas Turbine Combustors: A Review. *Hydrogen* **2021**, *2*, 33–57. [CrossRef]
49. Xiaoxiao, S.; Abbott, D.; Singh, A.V.; Gauthier, P.; Sethi, B. Numerical Investigation of Potential Cause of Instabilities in a Hydrogen Micromix Injector Array. In Proceedings of the ASME Turbo Expo 2021, Turbomachinery Technical Conference and Exposition, Virtual, 7–11 June 2021.
50. Cecere, D.; GCarpenella, S.; Giacomazzi, E.; Arcidiacono, N.; Di Nardo, A.; Antonelli, M. *Analisi di Meccanismi Chimici e Fluidodinamici in Fiamme Premiscelate Metano/Idrogeno/Aria*; Technical Report D2.2.5.1 of POR-H2 Project; ENEA: Stockholm, Sweden, 2023.
51. Altarawneh, M.; Saeed, A.; Al-Harahsheh, M.; Dlugogorski, B.Z. Thermal decomposition of brominated flame retardants (BFRs): Products and mechanisms. *Prog. Energy Combust. Sci.* **2019**, *70*, 212–259. [CrossRef]
52. Hayakawa, A.; Arakawa, Y.; Mimoto, R.; Somarathne, K.K.A.; Kudo, T.; Kobayashi, H. Experimental investigation of stabilization and emission characteristics of ammonia/air premixed flames in a swirl combustor. *Int. J. Hydrogen Energy* **2017**, *42*, 14010–14018. [CrossRef]
53. Cheong, P.; Chang, K.F.; Lai, Y.H.; Ho, S.K.; Sou, I.K.; Tam, K.W. A ZigBee-Based Wireless Sensor Network Node for Ultraviolet Detection of Flame. *IEEE Trans. Ind. Electron.* **2011**, *58*, 5271–5277. [CrossRef]
54. Djuric, Z.; Radulovic, K.; Trbojevic, N.; Lazic, A. Silicon resonant cavity enhanced UV flame detector. In Proceedings of the 2002 23rd International Conference on Microelectronics. Proceedings (Cat. No.02TH8595), Nis, Serbia, 12–15 May 2002; Volume 1, pp. 239–242. [CrossRef]
55. Pauchard, A.; Manic, D.; Flanagan, A.; Besse, P.; Popovic, R. A method for spark rejection in ultraviolet flame detectors. *IEEE Trans. Ind. Electron.* **2000**, *47*, 168–174. [CrossRef]
56. Starikov, D.; Boney, C.; Pillai, R.; Bensaoula, A. Dual-band UV/IR optical sensors for fire and flame detection and target recognition. In Proceedings of the ISA/IEEE Sensors for Industry Conference, New Orleans, LA, USA, 27–29 January 2004; pp. 36–40. [CrossRef]
57. Howell, J.; Siegel, R.; Menguc, M. *Thermal Radiation Heat Transfer*, 5th ed.; CRC Press: Boca Raton, FL, USA; Taylor & Francis Group: Oxford, NY, USA, 2010.

58. Modest, M.; Haworth, D. *Radiative Heat Transfer in Turbulent Combustion Systems*; Springer Briefs in Applied Sciences and Technology; Springer: Berlin/Heidelberg, Germany, 2016.
59. Caliot, C.; Flamant, G. Pressurized Carbon Dioxide as Heat Transfer Fluid: Influence of Radiation on Turbulent Flow Characteristics in Pipe. *AIMS Energy* **2014**, *3*, 172–182. [CrossRef]
60. Rothman, L.E.A. The HITRAN 2008 Molecular Spectroscopic Database. *J. Quant. Spectrosc. Radiat. Transf.* **2009**, *110*, 533–572. [CrossRef]
61. Rothman, L.; Gordon, I.; Barber, R.; Dothe, H.; Gamache, R.; Goldman, A.; Perevalov, V.; Tashkun, S.J.T. HITEMP, The High-Temperature Molecular Spectroscopic Database. *J. Quant. Spectrosc. Radiat. Transf.* **2010**, *111*, 2139–2150. [CrossRef]
62. Zhang, H.; Modest, M. Evaluation of the Planck–Mean Absorption Coefficients from HITRAN and HITEMP Databases. *J. Quant. Spectrosc. Radiat. Transf.* **2002**, *73*, 649–653. [CrossRef]
63. Kochanov, R.V. HITRAN Application Programming Interface (HAPI). User Guide. In *Harvard-Smithsonian Center for Astrophysics—Atomic and Molecular Physics Division*; Manual ver. 4.3; Atomic and Molecular Physics Division, Harvard-Smithsonian Center for Astrophysics: Cambridge, MA, USA, 2019
64. Wang, L.; Haworth, D.; Turns, S.; Modest, M. Interactions Among Soot, Thermal Radiation, and NOx Emissions in Oxygen-Enriched Turbulent Nonpremixed Flames: A CFD Modeling Study. *Combust. Flame* **2005**, *141*, 170–179. [CrossRef]
65. Wang, L.; Modest, M.; Haworth, D.; Turns, S. Modeling Nongray Soot and Gas-Phase Radiation in Luminous Turbulent Nonpremixed Jet Flames. *Combust. Theory Model.* **2005**, *9*, 479–498. [CrossRef]
66. Moss, J.; Stewart, C. Spectrally Resolved Measurements of Radiative Heat Transfer in a Gas Turbine Combustor. *Exp. Therm. Fluid Sci.* **2004**, *28*, 575–583. [CrossRef]
67. Ebara, T.; Iki, N.; Takahashi, S.; Park, W. Effect of Radiation Reabsorption on Laminar Burning Velocity of Methane Premixed Flame Containing with Steam and Carbon Dioxide. *JSME Int. J. Ser.-Fluids Therm. Eng.* **2006**, *49*, 260–264. [CrossRef]
68. Mercer, G.; Weber, R. Radiation Enhanced Combustion Wave Speeds. *Proc. R. Soc. Lond. A* **1997**, *453*, 1543–1549. [CrossRef]
69. Cecere, D.; Carpenella, S.; Quaranta, I.; Giacomazzi, E.; Sorrentino, G.; Sabia, P.; Ariemma, G. Large Eddy Simulation of Hydrogen/Air MILD combustion in a cyclonic burner. In Proceedings of the 10th Turbulence, Heat and Mass Transfer (THMT23), Rome, Italy, 11–15 September 2023.
70. Ripoll, J.F.; Pitsch, H. Modelling Turbulence-Radiation Interactions for Large Sooting Turbulent Flames. In *Annual Research Briefs*; Center for Turbulence Research, Stanford University: Stanford, CA, USA, 2002; pp. 41–52.
71. Turns, S. *An Introduction to Combustion: Concepts and Applications*, 3rd ed.; McGraw-Hill: New York, NY, USA, 2011.
72. Pisciotta, M.; Pilorge, H.; Feldmann, J.; Jacobson, R.; Davids, J.; Swett, S.; Sasso, Z.; Wilcox, J. Current state of industrial heating and opportunities for decarbonization. *Prog. Energy Combust. Sci.* **2022**, *91*, 100982. [CrossRef]
73. Wu, L.; Kobayashi, N.; Li, Z.; Huang, H. Experimental study on the effects of hydrogen addition on the emission and heat transfer characteristics of laminar methane diffusion flames with oxygen-enriched air. *Int. J. Hydrogen Energy* **2016**, *41*, 2023–2036. [CrossRef]
74. Michler, T.; Schweizer, F.; Wackermann, K. Review on the Influence of Temperature upon Hydrogen Effects in Structural Alloys. *Metals* **2021**, *11*, 423. [CrossRef]
75. Stefan, E.; Talic, B.; Gruber, A.; Peters, T.A. Materials challenges in hydrogen-fuelled gas turbines. *Int. Mater. Rev.* **2022**, *67*, 461–486. [CrossRef]
76. Min'ko, N.I.; Varavin, V.V. Effect of Water on the Structure and Properties of Glass (Review). *Glass Ceram.* **2007**, *64*, 3–6. [CrossRef]
77. Zier, M.; Stenzel, P.; Kotzur, L.; Stolten, D. A review of decarbonization options for the glass industry. *Energy Convers. Manag. X* **2021**, *10*, 100083. [CrossRef]
78. International Energy Agency. *CO_2 Emissions in 2022*; Technical Report; IEA: Paris, France, 2023.
79. Wrobel, K.; Wrobel, J.; Tokarz, W.; Lach, J.; Podsadni, K.; Czerwinski, A. Hydrogen Internal Combustion Engine Vehicles: A Review. *Energies* **2022**, *15*, 8937. [CrossRef]
80. Stepien, Z. A Comprehensive Overview of Hydrogen-Fueled Internal Combustion Engines: Achievements and Future Challenges. *Energies* **2021**, *14*, 6504. [CrossRef]
81. Faizal, M.; Chuah, L.; Lee, C.; Hameed, A.; Lee, J.; Shankar, M. Review of hydrogen fuel for internal combustion engines. *J. Mech. Eng. Res. Dev.* **2019**, *42*, 35–46.
82. Wang, J.; Huang, Z.; Fang, Y.; Liu, B.; Zeng, K.; Miao, H.; Jiang, D. Combustion behaviors of a direct-injection engine operating on various fractions of natural gas–hydrogen blends. *Int. J. Hydrogen Energy* **2007**, *32*, 3555–3564. [CrossRef]
83. Fayaz, H.; Saidur, R.; Razali, N.; Anuar, F.; Saleman, A.; Islam, M. An overview of hydrogen as a vehicle fuel. *Renew. Sustain. Energy Rev.* **2012**, *16*, 5511–5528. [CrossRef]
84. Heffel, J. NOx emission and performance data for a hydrogen fueled internal combustion engine at 1500 rpm using exhaust gas recirculation. *Int. J. Hydrogen Energy* **2003**, *28*, 901–908. [CrossRef]
85. Goldmeer, J. *Fuel Flexible Gas Turbines as Enablers for a Low or Reduced Carbon Energy Ecosystem*; Technical Report GEA33861; Electrify Europe: Vienna, Austria, 2018.
86. Wakayama, N.; Morimoto, K.; Kashiwagi, A.; Saito, T. Development of Hydrogen Rotary Engine Vehicle. In Proceedings of the World Hydrogen Energy Conference, Lyon, France, 13–16 June 2006.
87. AGORA. *Flexibility in Thermal Power Plants*; AGORA Energiewende: Berlin, Germany, 2017.

88. IRENA. *Power System Flexibility for the Energy Transition—Part 1: Overview for Policy Makers*; Technical Report; International Renewable Energy Agency: Masdar City, United Arab Emirates, 2018.
89. Gonzalez-Salazar, M.; Kirsten, T.; Prchlik, L. Review of the operational flexibility and emissions of gas- and coal-fired power plants in a future with growing renewables. *Renew. Sustain. Energy Rev.* **2018**, *82*, 1497–1513. [CrossRef]
90. Hiddemann, M.; Stevens, M.; Hummel, F. Increased Operational Flexibility from the GT26 (2011) Upgrade. In Proceedings of the Power-Gen Asia, Bangkok, Thailand, 3–5 October 2012.
91. Zuming, L.; Iftekhar, A. New operating strategy for a combined cycle gas turbine power plant. *Energy Convers. Manag.* **2018**, *171*, 1675–1684.
92. Prina, M.; Fanali, L.; Manzolini, G.; Moser, D.; Sparber, W. Incorporating combined cycle gas turbine flexibility constraints and additional costs into the EPLANopt model: The Italian case study. *Energy* **2018**, *160*, 33–43. [CrossRef]
93. Larfeldt, J. Technology options and plant design issues for fuel-flexible gas turbines. In *Fuel Flexible Energy Generation*; Woodhead Publishing: Thorston, UK, 2016; pp. 271–291.
94. Kido, H.; Nakahara, M.; Hashimoto, J.; Barat, D. Turbulent Burning Velocities of Two-Component Fuel Mixtures of Methane, Propane and Hydrogen. *JSME Int. J. Ser. B* **2002**, *45*, 355–362. [CrossRef]
95. Moccia, V.; D'Alessio, J. Characterization of CH4-H2-Air mixtures in the high-pressure DHARMA reactor. In Proceedings of the 25th International Conference on Efficiency, Cost, Optimization (ECOS), Perugia, Italy, 26–29 June 2012; pp. 287–503.
96. Tuncer, O.; Acharya, S.; Uhm, J. Dynamics and flashback characteristics of confined premixed hydrogen-enriched methane flames. *Int. J. Hydrogen Energy* **2009**, *34*, 496–506. [CrossRef]
97. AIAA. *Combustion Instabilities in Gas Turbine Engines: Operational Experience, Fundamental Mechanisms, and Modelling*; AIAA-Book, Progress in Astronautics and Aeronautics; American Institute of Aeronautics and Astronautics: Liston, FL, USA, 2005; Volume 210.
98. Abbott, D. Practical examples of the impact of variations in gas composition on gas turbine operation and performance. In Proceedings of the Gas to Power Europe Forum, Berlin, Germany, 23–25 January 2012.
99. Ferguson, D.; Richard, G.A.; Straub, D. Fuel Interchangeability for Lean Premixed Combustion in Gas Turbine Engines. In *Turbo Expo: Power for Land, Sea and Air*; Number ASME Paper No: GT2008-51261; ASME: New York, NY, USA, 2009; pp. 973–981.
100. Bruschi, R.; Giacomazzi, E.; Giulietti, E.; Stringola, C.; Nobili, M.; Pagliaroli, T.; Giammartini, S. An Optical Technique for the Identification and Tracking of Combustion Instabilities. In Proceedings of the 7th Mediterranean Combustion Symposium, Sardinia, Italy, 11–15 September 2011; The Combustion Institute: Pittsburg, PA, USA, 2011.
101. OXSENSIS. *Oxsensis Dynamic Pressure Measurement on a GE 9E Gas Turbine*; Technical Review OXC10041; OXSENSIS Ltd.: Oxfordshire, UK, 2020.
102. ETN Global. *Proposed NOx Emissions Reporting for Hydrogen-Containing Fuels*; ETN Position Paper; European Turbine Network: Brussels, Belgium, 2023.
103. Chiesa, P.; Lozza, G.; Mazzocchi, L. Using Hydrogen as Gas Turbine Fuel. *J. Eng. Gas Turbines Power* **2005**, *127*, 73–80. [CrossRef]
104. Ansaldo Energia. *Ansaldo Energia Solutions for Hydrogen Combustion: Fast-Forward to a Hydrogen Fueled Future*; Technical Report; Ansaldo Energia: Genoa, Itlay, 2021.
105. Clean Hydrogen Partnership. *Clean Hydrogen Joint Undertaking, Strategic Research and Innovation Agenda 2021–2027*; Annex to GB Decision no. CleanHydrogen-GB-2022-02; Technical Report; Hydrogen Europe: Brussels, Belgium, 2022.
106. ETN Global. *Hydrogen Gas Turbines—The Path Towards a Zero-Carbon Gas Turbine*; Technical Report; European Turbine Network: Brussels, Belgium, 2020.
107. Bothien, M.R.; Ciani, A.; Wood, J.P.; Fruechtel, G. Toward Decarbonized Power Generation With Gas Turbines by Using Sequential Combustion for Burning Hydrogen. *J. Eng. Gas Turbines Power* **2019**, *141*, 121013. [CrossRef]
108. Funke, H.H.W.; Beckmann, N.; Abanteriba, S. An overview on dry low NOx micromix combustor development for hydrogen-rich 735 gas turbine applications. *Int. J. Hydrogen Energy* **2019**, *44*, 6978–6990. [CrossRef]
109. Franco, A.; Giovannini, C. Routes for Hydrogen Introduction in the Industrial Hard-to-Abate Sectors for Promoting Energy Transition. *Energies* **2023**, *16*, 6098. [CrossRef]
110. TENOVA. *TSX SmartBurner Burning up to 100% Hydrogen*; Technical Report; TENOVA: Castellanza, Italy, 2020.
111. TENOVA. *Hydrogen-Ready SmartBurner for Heat Treatment Furnaces*; Technical Report; TENOVA: Castellanza, Italy, 2021.
112. LINDE. *REBOX Flameless Oxyfuel Technology*; Technical Report 31910_LCS_1017; LINDE AG, Gases Division: Dublin, Ireland, 2017.
113. von Scheele, J.; Zilka, V. Succesful Use of Flameless Oxyfuel in Steel Reheating. In Proceedings of the METAL 2020, Brno, Czech Republic, 20–22 May 2020.
114. Gomez, R.S.; Gomes, K.C.; Gurgel, J.M.A.M.; Alves, L.B.; Magalhães, H.L.F.; Queiroga, R.A.; Sousa, G.C.P.; Oliveira, A.S.; Vilela, A.F.; Silva, B.T.A.; et al. Investigating the Drying Process of Ceramic Sanitary Ware at Low Temperature. *Energies* **2023**, *16*, 4242. [CrossRef]
115. ARUP Kiwa. *Industrial Boilers—Study to Develop Cost and Stock Assumptions for Options to Enable or Require Hydrogen-Ready Industrial Boilers*; Study 285177-11; ARUP Group Limited: London, UK, 2022.
116. Wang, T.; Zhang, H.; Zhang, Y.; Wang, H.; Lyu, J.; Yue, G. Efficiency and emissions of gas-fired industrial boiler fueled with hydrogen-enriched nature gas: A case study of 108 t/h steam boiler. *Int. J. Hydrogen Energy* **2022**, *47*, 28188–28203. [CrossRef]
117. International Energy Agency. *The Future of Hydrogen, Sizing Today's Opportunities*; Report Prepared by the Iea for the f20, Japan; IEA: Paris, France, 2019.

118. AECOM. *Start-Up and Shut-Down Times of Power CCUS Facilities*; BEIS Research Paper, Summary of Study Report 2020/031; AECOM, Department for Business, Energy & Industrial Strategy: Tokyo, Japan, 2020.
119. International Energy Agency. *World Energy Outlook*; Technical Report; IEA: Paris, France, 2019.